

Leveraging Open Knowledge for Advancing Task Expertise in Large Language Models

Yuncheng Yang, Yulei Qin, Tong Wu, Zihan Xu, Gang Li, Pengcheng Guo, Hang Shao, Yucheng Shi, Ke Li, Xing Sun, Jie Yang, Yun Gu

Abstract—The cultivation of expertise for large language models (LLMs) to solve tasks of specific areas often requires special-purpose tuning with calibrated behaviors on the expected stable outputs. To avoid huge cost brought by manual preparation of instruction datasets and training resources up to hundreds of hours, the exploitation of open knowledge including a wealth of low rank adaptation (LoRA) models and instruction datasets serves as a good starting point. However, existing methods on model and data selection focus on the performance of general-purpose capabilities while neglecting the knowledge gap exposed in domain-specific deployment. In the present study, we propose to bridge such gap by introducing few human-annotated samples (i.e., K -shot) for advancing task expertise of LLMs with open knowledge. Specifically, we develop an efficient and scalable pipeline to cost-efficiently produce task experts where K -shot data intervene in selecting the most promising expert candidates and the task-relevant instructions. A mixture-of-expert (MoE) system is built to make the best use of individual-yet-complementary knowledge between multiple experts. We unveil the two keys to the success of a MoE system, 1) the abundance by K -shot, and 2) the insistence on diversity. For the former, we ensure that models that truly possess problem-solving abilities on K -shot are selected rather than those blind guessers. Besides, during data selection, instructions that share task-relevant contexts with K -shot are prioritized. For the latter, we highlight the diversity of constituting experts and that of the fine-tuning instructions throughout the model and data selection process. Extensive experimental results confirm the superiority of our approach over existing methods on utilization of open knowledge across various tasks. Codes and models will be released later.

Index Terms—Mixture of Experts, Low Rank Adaptation, Model Selection, Data Selection



1 INTRODUCTION

Recent few years have witnessed significant development of large language models (LLMs) across a broad spectrum of tasks and domains. The open-source community offers an array of competitive pre-trained/foundation models with general-purpose language understanding and generation capabilities [7], [36], [87], allowing for the follow-up special-purpose tuning customized for specific tasks and domains. To match specialist capabilities, one common exploration to boost pre-trained base models within specialty areas is instruction tuning on expert-curated contents [57], [71], [111]. However, such a training-intensive approach poses challenges to the manual collection and annotation of instruction-response pairs, which impedes agile development and deployment. On the other hand, extravagant computing resources are required to grasp the missing domain knowledge from scratch, making it difficult to appropriately calibrate for the expected responses.

Fortunately, a vast amount of fine-tuned and aligned models [95], together with instruction datasets across various domains and tasks [62], [92], [100], are available online. Such models often exist in the form of LoRA [32] adapters, which are derived from few strong base models. Given any task of interest, one

can choose pertinent models from the existing LoRA bank or library as a good starting point. Accordingly, researchers have developed various approaches to utilize and select the publicly released LoRA models [33], [63], [67] either in an off-line or an on-line manner for expeditious task adaptation. Meanwhile, great efforts have been put into the selection of high-quality open instruction datasets [74] for improving the instruction following capabilities, where the most challenging [15], [18], [48], [101] and influential [79], [98], [99], [109] datapoints are preferred.

Despite the tremendous progress made in model and data selection, most existing methods target at lifting LLMs for better alignment with human preference in general domains and common tasks. It remains an under-explored problem to advance specific task expertise of LLMs by fully exploiting the open knowledge such as public LoRA models and datasets. To fulfill such task-oriented knowledge augmentation, in this paper, we propose to bridge the gap between general and “vertical” domain knowledge by resorting to a few human-verified instruction samples (i.e., K -shot) from the task of interest. Such K -shot data play a steering role in guiding the selection of the most appropriate candidate models and beneficial datapoints to solve the task at hand.

Problem Definition Given a small amount of labeled, real-world instructions from the task of interest (K -shot), we aim at developing a universally effective and easily scalable pipeline that leverages publicly available models and datasets to advance the task expertise of state-of-the-art (SOTA) LLMs.

In this context, we encounter three primary challenges:

Challenge 1 Given a collection of LLMs including one foundation model and its fine-tuned LoRA variants, how can we take full advantage of K -shot to efficiently pinpoint the models with the highest potential for solving tasks of interest?

Y. Yang is with Institute of Image Processing and Pattern Recognition, Institute of Medical Robotics, Shanghai Jiao Tong University, Shanghai 200240, China, and Tencent YouTu Lab, Shanghai 200233, China (Email: yaphabates@sjtu.edu.cn).

Y. Qin, T. Wu, Z. Xu, G. Li, P. Guo, H. Shao, Y. Shi, K. Li, and X. Sun are with Tencent YouTu Lab, Shanghai 200233, China (Email: yuleiqin@tencent.com). J. Yang and Y. Gu are with Institute of Image Processing and Pattern Recognition, Institute of Medical Robotics, Shanghai Jiao Tong University, Shanghai 200240, China (Email: yungu@ieee.org).

Y. Yang and Y. Qin contributed equally.

Manuscript received Aug 25, 2024. Corresponding author: Yun Gu.

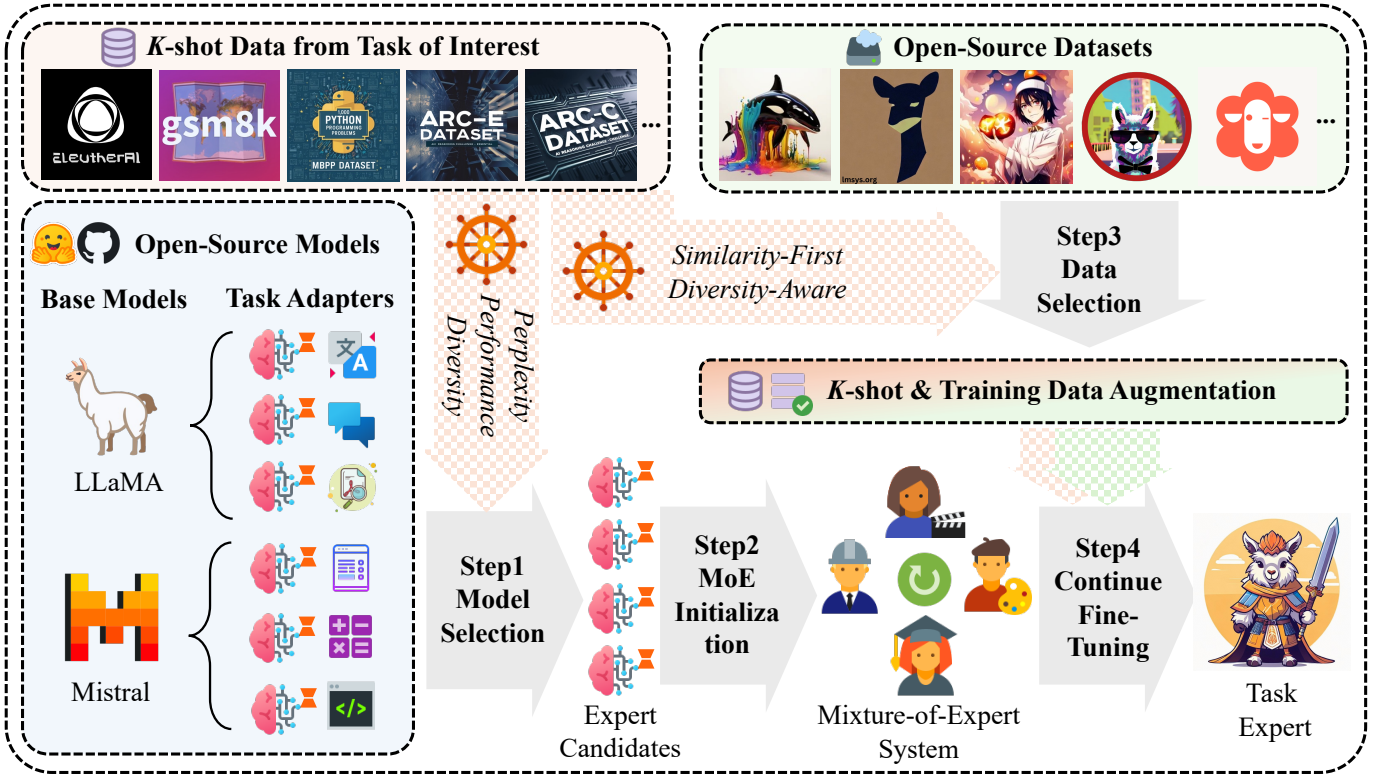


Fig. 1. Given few annotated data from any task of interest (K -shot), we aim to advance LLMs in task expertise by leveraging open-source models and datasets. We propose an efficient and scalable pipeline to fully exploit the steering role of K -shot throughout model and data selection. Highly promising experts are first selected from the model bank by comprehensive consideration of their perplexity and performance on the K -shot and intra-group diversity. These experts are initialized as one MoE system. Subsequently, we perform data augmentation by selecting diverse open instructions that resemble K -shot the most. Finally, we fine-tune the MoE system with both K -shot and the augmented data, which not only improves token-wise cooperation between experts but also integrates broad knowledge into the system. The ultimate task expert benefits from the complementary skills and knowledge of constituting experts.

Challenge 2 Given abundant instructions from open-source datasets, how can we identify the ones that share similar task or domain contexts with K -shot to inject supplementary knowledge into LLMs without causing overfitting?

Challenge 3 If multiple prospective LLMs are proved to be valid, how can we build an adaptive token-wise gating system to harness their individual-yet-complementary knowledge with improved cooperation between LLMs over K -shot?

To address these challenges, we propose the following task augmentation pipeline (see Fig. 1). Initially, for experimental control of comparability and reproducibility, we maintain our own LoRA bank by collecting thirty-eight representative open-source datasets and preparing a pool of LoRA models. It ensures the availability and diversity of instruction-tuned models on the basis of LLaMA [87] and Mistral [36] pre-trained models. Such a bank can be easily generalized to scenarios where all publicly released models are considered in practice. To tackle **Challenge 1**, we propose to select models that truly understand the task of interest rather than guessing randomly. We incorporate K -shot data to develop a selection mechanism featured by three key indicators: 1) reasoning perplexity: the uncertainty of a LLM in modeling the reasoning process towards its ultimate answer to each instruction; 2) exact match accuracy: the evaluation of the generated responses of the model on K -shot determined by the accuracy metric; 3) group diversity: the degree of distinction between multiple selected candidates measured in parameter versatility. To our best knowledge, the proposed method is the pioneering work that

uncovers K -shot for model selection where both the reasoning perplexity and the performance in accuracy provide insights into the generalized empirical risk of the model on examples from tasks of interest. We investigate and highlight the role of chain-of-thought (CoT) [93] reformulation of answers with rationales in improving the interpretability and robustness of perplexity as the expertise indicator. To address **Challenge 2**, we develop a similarity-first, diversity-aware data selection strategy for augmentation of task expertise, where K -shot intervene in retrieving the most similar open-source instructions in the embedding space. To bridge the knowledge gap between general- and special-purpose tasks without easily overfitting K -shot, we once again integrate diversity into the selection philosophy where semantic duplicates are removed to ensure a more dispersed distribution of datapoints. To resolve **Challenge 3**, we construct a mixture-of-experts (MoE) system and pay extra attention to the composition choice of experts at initialization and the token-wise coordination between experts in fine-tuning. For the former, we are the first study to demonstrate the critical role of a diversified selection of expert candidates in building a successful MoE system with open-source models. Such diversity effectively expands the knowledge boundary beyond a single model. For the latter, traditional methods either use linear model merging [34], [37], [106] or detached gating mechanism [63], [67], [84], neglecting the potential conflicts or sub-optimal allocation among experts. Their lack of interpretability further worsens generalization [102]. In contrast, our MoE system is fully optimized on K -shot data augmentation for mitigating

inter-expert conflicts and getting familiar with relevant tasks.

In summary, our contributions are four-fold:

- We propose a novel K -shot learning setting in forging LLMs with task expertise, where few human-verified instructions from tasks of interest are available for improving real-world applications in a cost-efficient way.
- We propose an effective and scalable pipeline that makes the best use of K -shot in leveraging open knowledge, where the most promising candidates and the most beneficial instructions are respectively selected from the public LoRA bank and the open-source datasets.
- We emphasize diversity throughout the proposed model and data selection strategies, which lays a solid foundation for constructing a versatile MoE system and acquiring task-relevant skills without overfitting.
- We demonstrate the advantages of a MoE system maximized by proper initialization and fine-tuning with enhanced domain knowledge and expert harmonization.

2 RELATED WORKS

2.1 Efficient Fine-tuning of Parameters

Parameter-efficient fine-tuning methods (PEFTs) are a set of techniques that diverge from traditional full-parameter fine-tuning. In PEFTs, only a certain subset of a model’s parameters are adjusted to better suit specific tasks of interest.

2.1.1 LoRA

Low-rank adaptation (LoRA) [32] and its variants [25], [54], [60], [110] use low-rank matrices to approximate additive weights during training. These methods are beneficial as they do not necessitate additional computational resources during inference, where the updated weights can be integrated into the model without any complications.

2.1.2 Prompt Tuning

Prompt-based methods incorporate randomly initialized soft tokens to the input, usually as a prefix, and train their embeddings while maintaining the LLM’s weights constant, as suggested in [44], [49], [118]. While these methods perform competitively, they do entail a substantial computational load during inference.

2.1.3 Adapters

Adapter methods involve the training of extra modules (for instance, fully connected layers) on top of the frozen pre-trained model [72], [117]. Unfortunately, these adapters are not effortlessly integrated into the original architecture, thereby reducing inference efficiency.

2.2 Mixture-of-Expert Models

The MoE technique [38], [83] combines several specialized expert models to efficiently scale up models for improved generalization. The principle behind MoE is that each expert is adept at handling a specific region of the input distributional space, and their combined decision-making outperforms any individual expert. Recent studies [29], [45], [50], [56], [97] focus on utilizing the MoE as a PEFT technique. Other methods [20], [33], [64], [67], [114] underscore the use of existing LoRA experts for convenient assembly, where the fine-tuning of their parameters is saved. Specifically, both [35] and [10] route to one expert by comparing

the input query with the averaged embeddings of the datasets used to train each individual expert. Such reliance on the fine-tuning datasets restricts the practicability of these methods. [28], [52], [58] all investigate external models such as GPT4 [3] and reward model [7] for estimation of the routing policy, which increases their cost of deployment and causes isolation between the routing model and the candidate experts. In spite of the development of merging techniques, few efforts [53], [69], [84] have been made to combine cross-domain experts for multi-task problems.

Very recently, PHATGOOSE [63] proposes a post-hoc adaptive token-wise gating mechanism to recycle from a collection of specialized experts. It aims at improving the zero-shot generalization of the pre-trained base model by constructing a routing system and performing dynamic token-by-token assignment. Despite the shared MoE principal, PHATGOOSE differs from the proposed method in three key aspects. First, the problem setting of PHATGOOSE is fundamentally different from ours in that they are not targeted at improving specific tasks of interest. There exists no model and data selection procedures in PHATGOOSE for acquiring task-relevant skills. Second, PHATGOOSE assumes that the contributors of the LoRA models provide additional gate modules that are implemented as sigmoid layers in front of each LoRA module. However, it is almost impossible to enforce the same gate training pipeline on the entire open-source community. In practice, one can only find the released LoRA modules from the repositories of Huggingface and Github without gating vectors. Third, our MoE system adapts to different tasks of interest by polishing the routing weights and the constituting experts simultaneously, while PHATGOOSE keeps the LoRA modules and gating vectors fixed with lower flexibility. Arrow [67] is another contemporary method which maintains the LoRA library and proposes a routing mechanism to select the most input-relevant LoRAs. Although Arrow is featured by its training-free routing, it does not consider the potential conflicts when the inputs are not representative enough of the given task. The statistics of the LoRA parameters (e.g., singular vectors) are directly used as the proxy for the routing weights, which is prone to be biased towards the original datasets used to train LoRA modules. Furthermore, they do not introduce the K -shot datapoints from downstream tasks for calibrating the expert behavior, and neglect the exploitation of open-source datasets for optimizing the expert collaboration.

2.3 Data Selection for Efficient Tuning

Existing methods on data selection for pre-training and instruction tuning of LLMs can be categorized into: 1) quality-based, 2) diversity-based, and 3) importance-based [74].

2.3.1 Quality

[59] explores perplexity, L2-Norm error, and memorization as quality scores to rank and prune pre-training corpora. [48] presents a novel self-guided approach to autonomously select high-quality samples from open-source datasets using the instruction-following difficulty (IFD) metric. [18] employs the GPT3.5 to score instruction-response pairs and filters out samples with scores below a threshold. [15] introduces instruct mining to automatically select high-quality instruction-following data for LLM fine-tuning. [27] proposes a quality evaluation model to extract high-quality subsets from the original dataset and designs an algorithm to further select a seed instruction dataset with extensive coverage.

2.3.2 Diversity

Geometry-based sampling methods are the most intuitive and widely-used ones for maximizing diversity of the selected samples [40], [82], [116]. In particular, k-center greedy [80] is favored in diversity sampling on massive pre-training and instruction-tuning corpus [11], [16], [27], [96]. It performs iterative and greedy selection on data that exhibit the most dissimilarity with the already selected set in the embedding space.

2.3.3 Importance

Two kinds of gradient-based methods on importance estimation have been developed: 1) gradient matching [8], [109], [113], i.e., the gradients of the entire set being approximated by the weighted gradients of the selected set, and 2) gradient influence [9], [13], [73], i.e., the influence of each training datapoint on the testing set being measured by upweighted gradient multiplication. For importance-oriented sampling, [99] adopts importance resampling to select a subset from a large-scale unlabeled dataset that shares similar distributions with the target set.

Although these methods strike a balance between data quality and quantity, they fail to incorporate the data selection pipeline into the task-oriented model development. On the contrary, the proposed method focuses on improving the downstream performance given limited K -shot real-word datapoints under the context of expert fusion. Correspondingly, we simultaneously consider the quality and importance where the resemblance of an open-source instruction to the K -shot set is prioritized during selection. In addition, we treasure the diversity of the selected dataset as its variety helps polish the coordination between experts in token-wise routing. To the best of our knowledge, the proposed method is the pioneer that integrates comprehensive data selection into the advancement of a MoE system for task expertise, where the concepts of quality, diversity, and importance play a critical role throughout the selection of both expert and data candidates.

3 METHODOLOGY

3.1 LoRA Bank Construction

The open-source community has witnessed a significant increase in the number of LoRA models and high-quality datasets. To ensure experimental reproducibility, rationality, and comparability, we have selected **thirty-eight** representative and widely-used instruction datasets from the Huggingface [95] to construct a rich and reliable LoRA bank.

3.1.1 Data Sources

Specifically, the data to construct our LoRA Bank are summarized as follows: ARC [22], Winogrande [1], GSM8K [23], PiQA [12], CommonSenseQA [85], RACE [42], MBPP [6], MathQA [5], Esnli [14], ECQA [4], CREAK [66], GPT4Tools [103], AQuA [51], QASC [39], QED [43], StrategyQA [30], SensemakingQA [89], Toolformer [78], HellaSwag [107], SiQA [77], BoolQ [21], Dolly [31], WizardLM [100], WebGPT [65], Lima [115], Code-Alpaca [91], ThoughtSource [68], CAMEL [46]. We choose these datasets for two reasons: 1) they provide a comprehensive coverage of mainstream tasks and domains, and 2) their quality is confirmed through massive downloads worldwide and positive feedback comments from researchers.

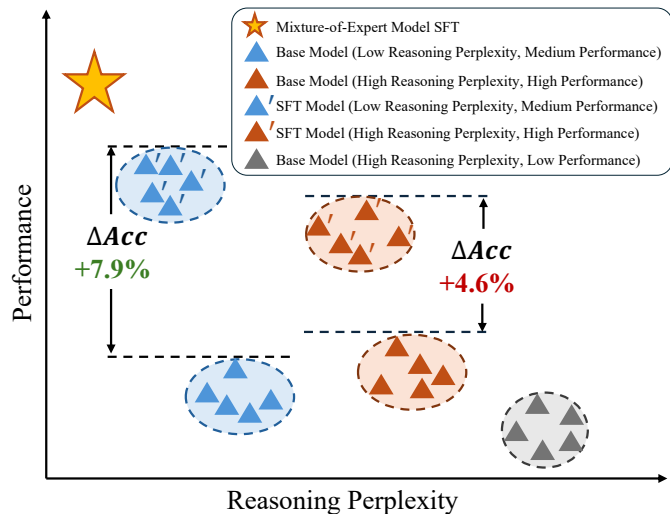


Fig. 2. The performance of task-specific fine-tuning versus the reasoning perplexity of candidate models in the bank. Preliminary experiments demonstrate that models of lower performance are not always in lack of domain-specific knowledge. Instead, their inability to follow instructions on the expected output format (e.g., answer choice) causes parsing failure during post-processing on the generated responses, which diminishes their performance in evaluation metrics. To avoid such biased, partial measurement merely by the exact-match accuracy, we propose to use the perplexity over the CoT rationales of answers as a superior, complementary proxy for model assessment. Accordingly, we evaluate if the model possesses the task-specific knowledge by computing its perplexity score of modeling the reasoning process. Models that achieve lower reasoning perplexity are considered competent and tend to achieve greater performance improvement after fine-tuning than those with higher reasoning perplexity.

3.1.2 Data Preprocessing

All raw datasets are processed into the following format: {"instruction": <instruction>, "input": <input (can be empty)>, "output": <output>}. For certain CoT datasets, we directly follow [75] to use the template from FLAN [57] and transform the original data into the data format above.

3.1.3 LoRA Fine-Tuning

For each dataset, we fine-tune pre-trained base models and derive their LoRA weights. These LoRA models are used for subsequent model selection. We follow [90] to set the hyper-parameters for optimization: a batch size of 2, gradient accumulation steps of 16, and an initial learning rate of 5e-5. Uniformly, all models underwent training for three epochs to ensure that each dataset is fully mastered regardless of the task difficulty. A cosine decaying schedule is adopted for adjusting the learning rate over iterations. The LoRA modules are applied on the linear embedding layers of the Query and Value matrices in self-attention. For all LoRAs, the rank was set to 16. To reduce training overhead, sequences with length exceeding 1024 were truncated.

3.2 K -shot Guided Expert Model Selection

In a bank of LoRA models, it becomes essential to appropriately select the most relevant task expert candidates [104], [105]. However, few studies have explored model selection options for language models, especially in the context of K -shot settings. Furthermore, K -shot labeled data are typically sparse and uniform in the input embedding space, which means that the evaluation

results of models on such limited data cannot reflect their true expertise level.

In this section, we propose to select highly-potential models that would perform well on any task of interest before conducting the task-specific fine-tuning. We hypothesize that two following perspectives should be prioritized during model selection: **1) Does the model possess the necessary knowledge for the tasks of interest?** and **2) Can the model adequately follow the instructions under the tasks of interest?** Accordingly, we first consider two indicators in estimation of the empirical risk on K -shot samples: 1) the specific evaluation metric for *performance* measurement, and the *perplexity* of a LLM in modeling the answers in an auto-regressive manner. Specifically, exact match accuracy is adopted in the present study as the default evaluation metric on the generated responses. If the answer choice precisely matches the model’s output, it is considered correct; otherwise, it is deemed incorrect. However, the empirical risk merely computed by performance is prone to be affected by poor instruction following capabilities of LLMs, where models that produce correct but unparseable answers are severely under-estimated. The post-processing techniques cannot handle all the corner cases of answers that are formatted unexpectedly. On the other hand, models that randomly guess the answer choices in QA tasks might be over-estimated. Such misjudgment originates from the low informative evaluation metric that fails to comprehensively assess whether the model can understand and handle the given task. Therefore, it calls upon the perplexity of the model on K -shot sequences as a straightforward complement. To reduce biased measurement merely from one indicator, we take into consideration of three aspects: 1) perplexity, 2) performance, and 3) diversity.

3.2.1 Perplexity

The perplexity of a LLM on auto-regressive modeling of the answers serve as an effective indicator of the model’s capability. Given a model m parameterized by θ_m , an input sequence x , and its expected output sequence y , the perplexity of language modeling is defined with cross-entropy:

$$\text{PPL}(x, y, \theta_m) = \exp\left(-\sum_{i=1}^{|y|} \log P(y_{(i)}|x, y_{(<i)}; \theta_m)\right), \quad (1)$$

where $P(y_{(i)}|x, y_{(<i)})$ is the predicted probability of the i -th token $y_{(i)}$ of y given the sequences x and $y_{(<i)}$.

However, as explained in the drawbacks of exact match on multiple-choice problems, the perplexity computed solely on the ground-truth answer options in many QA tasks still suffers from inaccurate estimation of model capabilities. To address this issue, we utilized an advanced open model [61] to expand the answers with CoT rationales. Subsequently, we calculated the reasoning perplexity of LoRA models by considering both the predicted answer choices and the rationales behind them:

$$\text{PPL}(x, \hat{y}, \theta_m) = \exp\left(-\sum_{i=1}^{|\hat{y}|} \log P(\hat{y}_{(i)}|x, \hat{y}_{(<i)}; \theta_m)\right), \quad (2)$$

$$\hat{y} = \Phi(x, y), \quad (3)$$

where $\Phi(x, y)$ represents the CoT expansion process given both the input x and the output y . For such CoT rationales, we target at multiple-choice datasets whose outputs are only answer options (e.g., A and B). We use the CoT-formatted answers rewritten by

Prompt Template to Generate CoT Rationales

Read the question and answer. According to the answer, present your thought about the solution.

- Please think step by step and provide the answer first then with its explanation.
- Your explanation should not exceed three sentences.

Question: {Question}

Answer: {Answer}.

Fig. 3. Expansion of the CoT rationales on K -shot instructions.

the WizardLM2-8x22B [61] for reasoning explanations (see Fig. 3 for detailed prompts). Such rationales improve the transparency and interpretability of the decision-making process, which benefits accurate model selection by estimating the uncertainty of any LLM on the rationales under the context of instruction. Besides, answers with reasoning process in advance are more effective in fine-tuning models, where the justified rationales well calibrate the response towards the ultimate correct answers. As illustrated in Fig. 2, models with higher reasoning perplexity might achieve better performance before task-specific tuning, but their performance gains brought by fine-tuning are not as strong as models with lower reasoning perplexity.

For the K -shot $D_K = \{(x_1, y_1), (x_2, y_2), \dots, (x_K, y_K)\}$, $|D_K| = K$, the total *reasoning perplexity* is defined as:

$$\text{PPL}_R(m, D_K) = \sum_{(x_i, y_i) \in D_K} \text{PPL}(x_i, \Phi(x_i, y_i), \theta_m). \quad (4)$$

3.2.2 Performance

The evaluation metric measured on K -shot directly reflects a model’s ability to solve the corresponding task in an “end-to-end” way. We denote such evaluation results as the *performance*, which is defined by any metric calculated by comparing the generated responses \tilde{y} and the ground-truth answers y . In line with the task requirement, a post-processing step might be involved to extract formatted answers from responses. It can be implemented through certain function $f(\cdot)$, i.e., $\tilde{y}' = f(\tilde{y})$. Common post-processing operations include threshold-based truncation and probability-to-category mapping. Out of simplicity, the performance of a model m on the dataset D_K can be defined as the accuracy of matching the post-processed \tilde{y}' with the ground-truth y :

$$\text{Acc}(m, D_K, f) = \frac{1}{N} \sum_{(x_i, y_i) \in D_K} \mathbb{1}(\tilde{y}'_i = y_i), \quad (5)$$

$$\tilde{y}'_i = f(\tilde{y}_i),$$

where $\mathbb{1}(\cdot)$ is the indicator function that equals to 1 when the condition holds true and 0 otherwise. \tilde{y}_i is the predicted response by θ_m given the input x_i .

3.2.3 Diversity

To fully harness the task-related knowledge inherent in models from the LoRA Bank, our objective is to select all candidate models that are likely to solve the downstream tasks. To expand the knowledge base, it is essential to “deduplicate” the selected models so that each candidate model contributes to the accumulation of skills. Therefore, diversity is ensured so that different

selected experts possess distinct abilities. Contrary to existing studies [41], [47], [84] that primarily focus on combining experts without considering their relationships, we highlight the concept of *group diversity* for retrieving expert candidates. It refers to the variety of the selected models in a group. A high intra-group diversity lays a solid foundation for exploitation of task-relevant yet complementary knowledge. Given a group of N expert models $B_N = \{m_1, m_2, \dots, m_N\}$, the group diversity Ω_{B_N} is defined as the inverse of the sum of cosine similarities between the parameters of each model pair $\mathbf{E}(m_i)$ and $\mathbf{E}(m_j)$:

$$\Omega_{B_N} = \left(\frac{2}{N(N-1)} \sum_{m_i \in B_N} \sum_{m_j \neq m_i} \frac{\mathbf{E}(m_i) \cdot \mathbf{E}(m_j)}{\|\mathbf{E}(m_i)\| \|\mathbf{E}(m_j)\|} \right)^{-1}, \quad (6)$$

where $\mathbf{E}(m_i)$ denotes the flattened matrices of layers in the model m_i . The cosine similarity between the paired m_i and m_j is computed matrix by matrix and averaged over all layers.

3.2.4 Selection Mechanism

The overall pipeline of model selection is illustrated in Fig. 4 and detailed in Alg. 1. One important principle behind our pipeline design is to comprehensively employ indicators from various aspects, which reduces the bias by partial measurement.

We first calculate the reasoning perplexity and the performance in accuracy for each model in the bank B based on Eq. 4 and Eq. 5. We sort models by perplexity and performance respectively from smallest to largest and from largest to smallest. The rankings by perplexity and performance are respectively denoted as R_P and R_A . Then, we select M candidate models B_M^* from the LoRA Bank B with minimum sum of rankings R_P and R_A . In this way, models in lack of task-relevant knowledge and skills are filtered out in advance to greatly reduce the computation overhead on diversity measurement. Subsequently, we calculate the group diversity Ω_{B_N} on all combinations of N -tuples B_N from B_M^* , and sort these tuples by intra-group diversity from largest to smallest for the ranking R_D . Finally, we sum up all the rankings of R_P , R_A , and R_D and choose the top N models $B_N^* \subset B_M^*$, $|B_N^*| = N$ for initializing our MoE system B_E .

Compared with other methods, our selection approach is more robust to variation of K -shot across tasks due to its all-sided evaluation in perplexity, performance, and diversity. Besides, it consumes fewer computational resources for two reasons: 1) Low-quality and impotent models are eliminated before the exhaustive computation of intra-group diversity. 2) Each model performs evaluation only once on K -shot data.

3.3 Mixture-of-Experts Initialization

Upon selecting the most promising experts, our objective is to efficiently utilize their potentials at respective domains. The linear arithmetic composition offers a straightforward approach to benefit from our LoRA bank [20], [33], [108]:

$$\hat{\mathbf{W}} = \mathbf{W} + \sum_{i=1}^N w_i \Delta \mathbf{W}_i, \quad (7)$$

where \mathbf{W} indicates the original parameter of a pre-trained model and $\Delta \mathbf{W}_i$ denotes the i -th LoRA variant with $\sum_{i=1}^N w_i = 1$. Nevertheless, such a naive method of assigning weights to different LoRAs does not promise a dynamic and flexible routing mechanism, restricting its quick adaptation to any task of interest.

Algorithm 1 K -shot Guided Expert Model Selection

Input: A model bank B , number of candidate models M , number of selected experts N , K -shot data D_K , and post-processing function $f(\cdot)$

Output: Selected experts B_E

- 1: Compute the reasoning perplexity $\text{PPL}_R(m, D_K)$ and the performance by accuracy $\text{Acc}(m, D_K, f)$ for $\forall m \in B$
 - 2: **for all** $m \in B$ **do**
 - 3: Extract the ranking $R_P(m) \leftarrow \text{rank}(\text{PPL}_R(m, D_K))$ by sorting from smallest to largest
 - 4: Extract the ranking $R_A(m) \leftarrow \text{rank}(\text{Acc}(m, D_K, f))$ by sorting from largest to smallest
 - 5: **end for**
 - 6: Find the top M models B_M with the smallest sum of rankings in both perplexity and performance
 $B_M^* \leftarrow \arg \min_{B_M \subset B, |B_M|=M} \sum_{m \in B_M} (R_P(m) + R_A(m))$
 - 7: Calculate the group diversity Ω_{B_N} for all N -tuples $\forall B_N \subset B_M, |B_N| = N$
 - 8: **for all** $B_N \subset B_M$ **do**
 - 9: Extract the ranking $R_D(B_N) \leftarrow \text{rank}(\Omega_{B_N})$ by sorting from largest to smallest
 - 10: **end for**
 - 11: Find the N -tuple $B_N \subset B_M, |B_N| = N$ with the smallest sum of rankings in perplexity, performance, and group similarity
 $B_N^* \leftarrow \arg \min_{B_N \subset B_M^*, |B_N|=N} \sum_{m \in B_N} (R_P(m) + R_A(m)) + R_D(B_N)$
 - 12: **return** $B_E = B_N^*$
-

A more reasonable strategy would be a mixture of expertise. Specifically, we train the router in such a manner that the model autonomously allocates different tokens to appropriate experts. Given an input x , the output of a N -expert MoE system at the l -th layer $g^l(x)$ is computed as the weighted sum of the outputs from each expert:

$$g^l(x) = \sum_{i=1}^N G_i^l(x) \cdot g_i^l(x), \quad (8)$$

where $G_i^l(x)$ represents the i -th element of the gating vector $G^l(x) \in \mathbb{R}^N$, controlling the contribution of the i -th expert. $g_i^l(x)$ is the output from the i -th expert at the l -th layer. A simple yet efficient implementation of the gating network $G^l(\cdot)$ is a single fully-connected layer W_g^l , where the gating vector is obtained by matrix multiplication between W_g^l and $g_i^l(x)$. Only the top- k activated experts are selected with their gating weights re-normalized via softmax function:

$$G^l(x) = \text{softmax} \left(\text{top-}k \left(g_i^l(x) \cdot W_g^l \right) \right), \quad (9)$$

where $\text{top-}k(\cdot)$ keeps the value of the largest k elements unchanged and returns the other elements as $-\infty$. We fine-tune all LoRA experts and routers simultaneously (see Fig. 5).

3.4 K -shot Guided Sim-Div Data Selection

In situations where few annotated data are available under the task of interest, it is prone to overfitting if our MoE system is directly fine-tuned on these datapoints. A common approach to address this issue is data augmentation [26], [81], [94], [112], which mitigates

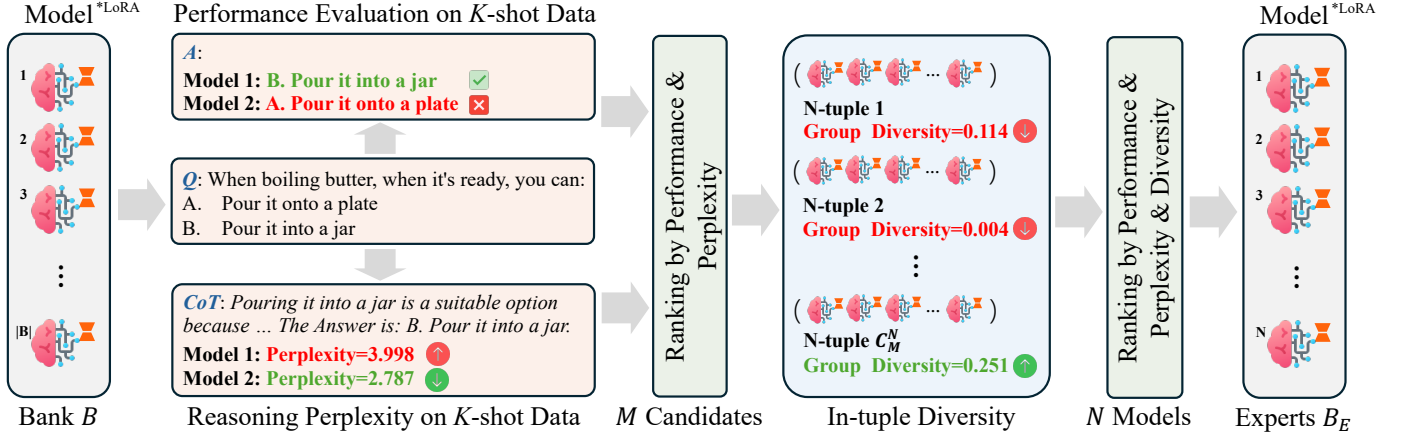


Fig. 4. The overall pipeline of our K -shot guided model selection strategy. A comprehensive assessment in terms of perplexity, performance, and diversity is conducted on each model for expert selection. Given K -shot data, we evaluate a model’s performance via exact match accuracy on the directly inferred results. The reasoning perplexity is obtained by computing the perplexity on auto-regressive modeling of the CoT rationales towards answers of K -shot. The top- M ranked candidate models are first selected to save computation of the subsequent intra-group diversity, where every N -tuple out of the M candidates are involved. The N models that share the lowest similarity in parameters (i.e., the largest group diversity) contribute to the initialization of a MoE system.

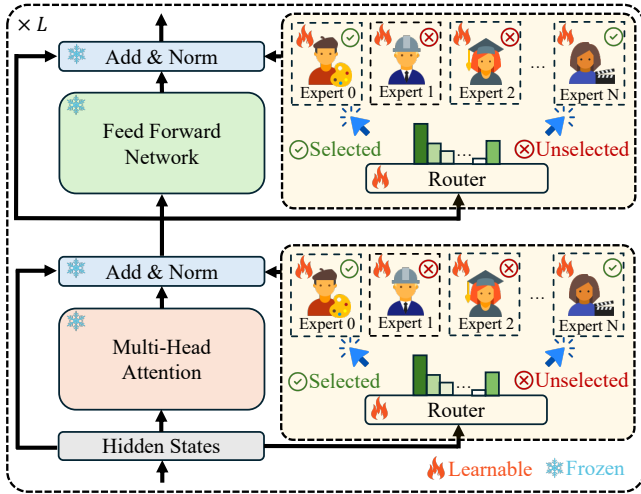


Fig. 5. The architecture of our MoE system. It is implemented with LoRA modules, where the selected models from the LoRA bank are trained with an additional router to learn to assign different tokens to the responsible experts. Each token is routed to the top- k activated experts with their representations multiplied by the corresponding routing weights for normalization.

the risk of degeneration via lexical or semantic augmentation on the original text inputs. Such manually designed techniques tend to work on traditional discriminative models by imposing perturbations to the decision boundary. However, for generative LLMs, vanilla data augmentation methods do not inherently inject any new knowledge into the model, nor do they fundamentally improve the diversity of the maintained instruction dataset.

In the light of this statement, we propose to leverage open-source data for task-oriented augmentation. It has three advantages including: 1) high cost-efficiency of utilizing the massive and free open-source datasets, 2) prevention of overfitting by introducing diverse and beneficial instructions, and 3) improvement of token-wise collaboration between experts via acquiring novel knowledge. When it comes to the selection of specific data instances, a new question is raised: **What type of open-source data should**

be favored to improve the performance on our task of interest?

In the present study, we assume that datapoints that share a similar distribution with samples in the downstream tasks ought to be prioritized. Accordingly, we propose the similarity-first and diversity-aware principle to guide the data selection process.

3.4.1 Data Encoding

In the first step, we perform encoding of the raw instruction texts for their projection into the embedding space. Given the K -shot D_K and a set of S open-source samples $D_S = \{(x_1, y_1), (x_2, y_2), \dots, (x_S, y_S)\}, |D_S| = S$, we aim to find the most relevant datapoints in D_S based on their similarity with samples in D_K . Given a pre-trained encoding model h parameterized by θ_h , we obtain the representation of each sample u_i with both input and output via:

$$u_i = h([x_i, y_i]; \theta_h), \tag{10}$$

where $[\cdot, \cdot]$ denotes the concatenation operation in python syntax. The embeddings of samples (x_i, y_i) from D_K and D_S are respectively denoted as U_K and U_S . In practice, we employ the pre-trained BGE model [17] as h , which is fine-tuned on the XLM-RoBERTa [24] with self-distillation on corpus of multiple languages, tasks, and granularities. Specifically for extraction of u_i , we use the prefix prompt of `query_instruction_for_retrieval`: “Represent the following sentence for similar task retrieval: $\langle [x_i, y_i] \rangle$ ”.

3.4.2 Similarity-First

We calculate the cross-dataset similarity between D_K and D_S to select a subset $D_C \subset D_S$ that resembles D_K the most. First, we define a distance $d(\cdot, \cdot)$ to measure the similarity between two encoded samples u_i and u_j . Without losing generality, we demonstrate an intuitive implementation of similarity metric via cosine distance:

$$\text{sim}(u_i, u_j) = 1 - d_{\text{cos}}(u_i, u_j) = \frac{u_i \cdot u_j}{\|u_i\| \|u_j\|}, \tag{11}$$

where each pair of $u_i \in U_K$ and $u_j \in U_S$ constructs the entry A_{ij} of the similarity matrix $A \in \mathbb{R}^{K \times S}$:

$$A_{ij} = \text{sim}(u_i, u_j). \tag{12}$$

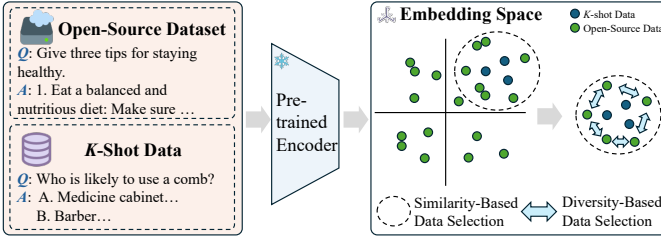


Fig. 6. The overall pipeline of our K -shot guided sim-div data selection. We extract the embeddings of both K -shot and open-source data through pre-trained models. In the embedding space, samples that are close to K -shot are identified and prioritized for task augmentation. Simultaneously, to ensure data diversity, we remove batches of data with near-duplicate semantics.

Then, we pinpoint top C samples in D_S that share the most similarity with D_K by maximizing along the rows of A :

$$D_C^* = \arg \max_{D_C \subset D_S, |D_C|=C} \sum_{(x_j, y_j) \in D_C} (\max_i A_{ij}). \quad (13)$$

The reasons why D_C is first selected out of D_S are two-fold: 1) It ensures that the samples which enjoy a high level of similarity with D_K are prioritized while those dissimilar ones would not be unexpectedly introduced into the candidate set during the subsequent selection. 2) It reduces the computation overhead of diversity measurement since the entire set D_S shrinks into a much smaller candidate set D_C with $C \ll S$.

3.4.3 Diversity-Aware

We remove duplicates in D_C to improve its overall diversity for the selected dataset D_A . A greater level of diversity not only improves the token-wise cooperation between experts on broader domains and topics but also reduces the overfitting of the MoE system on K -shot datapoints. Specifically, we remove a subset of data with excessively high semantic similarity. We use the same distance metric defined in Eq. 11 and compute the intra-dataset similarity matrix I . The pairwise similarity is measured on both $u_i \in U_C$ and $u_j \in U_C$, where $U_C = \{u_i | (x_i, y_i) \in D_C\}$:

$$I_{ij} = \text{sim}(u_i, u_j). \quad (14)$$

We follow the SemDeDup [2], [86] to perform semantic deduplication by thresholding with τ . If the similarity between any two instructions exceeds τ , we discard the one whose similarity with K -shot D_K is lower. By this means we maintain the overall diversity of the final selected dataset D_A . The entire process of data selection is elaborated in Alg. 2.

3.5 Mixture-of-Experts Fine-Tuning

We combine the augmented dataset D_A and the K -shot dataset D_K for optimizing both the routing weights and the experts of our MoE system θ_{MoE} , where the cross-entropy loss is employed to supervise the language modeling on the outputs of the last L -th MoE layer (Eq. 8):

$$\mathcal{L}(x, y, \theta_{\text{MoE}}) = - \sum_{i=1}^{|y|} \log P(y_{(i)} | x, y_{(<i)}; \theta_{\text{MoE}}), \quad (15)$$

where $P(y_{(i)} | x, y_{(<i)}; \theta_{\text{MoE}}) = \text{softmax}(g^L([x, y_{(<i)}]))_{y_{(i)}}$.

Algorithm 2 K -shot Guided Sim-Div Data Selection

Input: A set of open-source instruction samples D_S , K -shot data D_K , encoding model h , pairwise similarity metric $\text{sim}(\cdot, \cdot)$, data budget C , and similarity threshold τ

Output: Augmented dataset D_A

- 1: Encode each $(x_i, y_i) \in D_S$ and $(x_j, y_j) \in D_K$ by h respectively for the embedding sets of U_S and U_K
- 2: Compute the cross-dataset similarity matrix between D_K and D_S as $A \in \mathbb{R}^{K \times S}$, where $A_{ij} = \text{sim}(u_i, u_j), u_i \in U_K, u_j \in U_S$
- 3: Find the top C datapoints in D_S that share the highest similarity with samples in K -shot D_K
 $D_C^* = \arg \max_{D_C \subset D_S, |D_C|=C} \sum_{(x_j, y_j) \in D_C} (\max_i A_{ij})$
- 4: Compute the intra-dataset similarity matrix within D_C as $I \in \mathbb{R}^{C \times C}$, where $I_{ij} = \text{sim}(u_i, u_j), u_i \in U_C, u_j \in U_C, U_C = \{u_i | (x_i, y_i) \in D_C\}$
- 5: **for all** $(x_i, y_i) \in D_C, (x_j, y_j) \in D_C, i \neq j$ **do**
- 6: **if** $I_{ij} > \tau$ **then**
- 7: **if** $\max_r A_{ri} > \max_r A_{rj}$ **then**
- 8: $D_C \leftarrow D_C \setminus \{(x_j, y_j)\}$
- 9: **else**
- 10: $D_C \leftarrow D_C \setminus \{(x_i, y_i)\}$
- 11: **end if**
- 12: **end if**
- 13: **end for**
- 14: **return** $D_A = D_C$

4 EXPERIMENTS

4.1 Experiments Setup

In this section, we validate the effectiveness of our proposed method through a series of experiments on various tasks of interest. To begin with, we use six popular open-source datasets, namely ARC-Challenge, ARC-Easy [22], PiQA [12], BoolQ [21], MBPP [6], and GSM8K [23], to serve as our evaluation sets under tasks of interest. These datasets cover a diverse range of fields, including examination, knowledge question-answer (QA), common sense reasoning, mathematical problems, and code generation. For each dataset, we randomly sample K labeled instruction-response pairs from its official training set as K -shot. In consideration of the response format, we employ a post-processing approach customized for each task to standardize the outputs for fair comparison. For examination and QA datasets in the LoRA bank whose ground-truth answers are multiple-choices, we implement the rationale expansion and train the corresponding LoRA models on the CoT-formatted answers for improved task comprehension. Details about the datasets and the performance of each LoRA model can be found in the supplementary materials.

To enhance the performance of our MoE system, we employ data augmentation by introducing additional datasets for data selection and MoE fine-tuning (see Secs. 3.4 and 3.5). Specifically, CommonSenseQA [85] and SiQA [77] are involved for multiple-choice QA tasks (ARC-Challenge, ARC-Easy, PiQA, and BoolQ). We choose CommonSenseQA and SiQA in data augmentation for two reasons: 1) they share the same output formats with the downstream tasks in the testing sets; 2) they span a wide variety of common knowledge and social situations. While for code generation (MBPP) and mathematical reasoning (GSM8K) tasks, we choose WizardLM [100] because the dataset itself claims to be effective in improving LLMs in solving coding and maths

TABLE 1

Comparison with baselines and SOTA methods on six downstream tasks. The D_K , D_A , and D_T respectively denote the K -shot data, the selected open-source data for augmentation, and the entire training set of the downstream tasks.

Model	Method	MoE	K -shot	External	ARC-c	ARC-e	BoolQ	PiQA	GSM8K	MBPP	Avg.
LLaMA2-7B	Base Model	×	×	×	33.90%	49.91%	47.86%	53.05%	16.68%	18.20%	36.60%
	Random	×	D_K	×	40.11%	58.42%	60.12%	55.47%	18.53%	20.00%	42.11%
	Expert LoRA	×	D_T	D_T	44.07%	62.61%	63.39%	56.58%	22.88%	22.40%	45.32%
	Source Best	×	×	×	49.49%	69.31%	65.81%	61.53%	22.88%	24.60%	48.94%
	Source Best SFT	×	D_K	D_A	55.13%	72.14%	68.91%	64.32%	23.82%	24.40%	51.45%
	MixLoRA [45]	✓	D_K	×	41.24%	57.92%	60.56%	54.79%	18.53%	20.20%	42.21%
	LoRAHub [33]	✓	D_K	×	43.01%	57.43%	62.91%	53.12%	19.34%	23.80%	43.27%
	PEMs [108]	✓	D_K	D_A	50.12%	69.43%	67.12%	63.21%	19.83%	24.00%	48.95%
	Ours	✓	D_K	D_A	57.76%	73.60%	69.45%	65.13%	24.83%	24.20%	52.50%
	Mistral-7B	Base Model	×	×	×	60.68%	73.54%	55.96%	57.67%	45.56%	36.00%
Random		×	D_K	×	68.81%	81.31%	69.30%	66.97%	47.54%	36.80%	61.79%
Expert LoRA		×	D_T	D_T	77.97%	90.30%	80.12%	68.12%	49.73%	37.60%	67.31%
Source Best		×	×	×	80.00%	90.30%	80.12%	71.76%	51.55%	40.60%	69.06%
Source Best SFT		×	D_K	D_A	78.43%	88.76%	83.29%	76.01%	52.43%	40.00%	69.82%
MixLoRA [45]		✓	D_K	×	69.15%	83.42%	74.53%	67.93%	48.67%	37.80%	63.58%
LoRAHub [33]		✓	D_K	×	69.21%	84.14%	80.24%	65.31%	47.94%	39.60%	64.41%
PEMs [108]		✓	D_K	D_A	79.84%	89.87%	87.41%	74.07%	48.43%	39.60%	69.87%
Ours		✓	D_K	D_A	81.43%	92.29%	89.71%	78.89%	52.91%	41.40%	72.77%

problems. The selection of open-source data for augmentation adheres to the principle that **no data leakage** occurs with respect to the testing sets. The availability and quality of these datasets are guaranteed according to the feedback from developers in the community. In total, a mixture of K -shot data from downstream tasks and the selected data from open-source datasets are utilized for fine-tuning our MoE system.

4.2 Implementation Details

For preparation of 38 models in our LoRA bank, both LLaMA2-7B (Base) [87] and Mistral-7B (Base) [36] are investigated in the present study. We empirically set the number of candidate models $M = 8$, the number of chosen experts $N = 4$, and the number of selected experts $k = 2$. By default, we set $K = 50$ for K -shot data. Due to the randomness of sampling K -shot as the seed instructions, we perform sampling three times and report the averaged experimental results with three different sets of K -shot to ensure the reliability of testing. For data augmentation, the total number of open-source samples S is respectively 43K and 143K for the combined CommonSenseQA and SiQA, and the WizardLM. By default, the data budget C is set to 1K and the similarity threshold is $\tau = 0.9$. During experiments, we set the hyper-parameters following [90] for training the MoE system: a batch size of 2, gradient accumulation steps of 16, and a learning rate of $5e-5$. We fine-tune all MoE models for five epochs and their convergence is guaranteed. We do not observe further benefits with longer training. For all LoRA models incorporated in the LoRA Bank, the rank was set to 16. To optimize memory utilization, the employed training setting was the DeepSpeed [76] zero stage 3. All models were trained with PyTorch [70] Transformers [95] (version 4.36.1) on NVIDIA V100 GPUs with Float16 mode.

Explanations on all the symbols and the settings of all hyper-parameters can be found in the supplementary materials.

4.3 Baselines

We compare the proposed method with five vanilla baselines: 1) the pre-trained base (Base Model), 2) the randomly selected model from the LoRA bank fine-tuned only on K -shot data (Random) 3) the base model respectively fine-tuned on the entire training set

D_T of each task of interest (Expert LoRA), 4) the expert in the LoRA bank that achieves the best evaluation results respectively on the testing set of each downstream task (Source Best), and 5) each source best expert fine-tuned on the same augmented open datasets with ours (Source Best SFT). It is noted that baselines of Random, Expert LoRA, Source Best, and Source Best SFT are optimized task-by-task, and therefore their results on each individual task are reported respectively. Note that for the Random method, random sampling is performed three times and results are averaged over three fine-tuned models.

Furthermore, we compare with several SOTA methods including: 1) training a MoE system with randomly initialized LoRA models and routers (MixLoRA) [45], 2) combining pre-trained LoRA models and fine-tuning only the routers with K -shot data (LoRAHub) [33], 3) performing model merging and fine-tuning on LoRA models (PEMs) [108]. All these methods unearth available LoRA models for maximizing the generalization of LLMs either on unseen domains and tasks or under task-specific supervised scenarios. Out of comparability, we implemented SOTA methods with their officially released codes. We adopted the same hyper-parameter settings with ours for these methods except LoRAHub, where its default hyper-parameters are kept unchanged.

4.4 Results on Tasks of Interest

4.4.1 Comparison with Baselines

The experimental results can be found in Table 1. The comparison between LoRA and MixLoRA is straightforward, as it highlights the importance of our model selection. The rational use of open-source knowledge for specific tasks proves to be superior to the single LoRA and the vanilla mixing policy in MixLoRA. LoRAHub is a scheme that also maintains an open-source knowledge base. PEMs is a strategy that directly merges model parameters, which is intuitive but lacks rationality. In addition, these methods rarely consider the impact of the diversity between experts on the overall system. Our method outperforms existing approaches, showcasing its effectiveness.

4.4.2 Visualization of Experts

The activation patterns of individual experts are illustrated in Fig. 7. For each layer, we calculate the average activation rate

TABLE 2

Ablation study on the model selection strategy for initialization of the MoE system. The R_P , R_A , and R_D respectively represent the ranking by reasoning perplexity, the ranking by performance in accuracy, and the ranking by group diversity.

Model	Method	MoE	Perp-lexity	Perfor-mance	Group Diversity	ARC-c	ARC-e	BoolQ	PiQA	GSM8K	MBPP	Avg.
LLaMA2-7B	Base Model	×	×	×	×	33.90%	49.91%	47.86%	53.05%	16.68%	18.20%	36.60%
	Random	✓	×	×	×	47.81%	63.42%	64.19%	55.26%	17.87%	22.40%	45.16%
	Ours	✓	R_P	×	×	54.32%	68.54%	69.71%	63.39%	23.71%	24.00%	50.61%
		✓	×	R_A	×	55.16%	69.32%	66.15%	62.32%	23.71%	24.00%	50.11%
		✓	R_P	R_A	×	54.64%	71.94%	67.99%	65.32%	23.49%	23.40%	51.13%
✓	R_P	R_A	R_D	57.76%	73.60%	69.45%	65.13%	24.83%	24.20%	52.50%		
Mistral-7B	Base Model	×	×	×	×	60.68%	73.54%	55.96%	57.67%	45.56%	36.00%	54.90%
	Random	✓	×	×	×	76.51%	84.41%	85.03%	70.99%	47.83%	39.00%	67.29%
	Ours	✓	R_P	×	×	79.32%	89.31%	86.91%	75.14%	49.37%	40.40%	70.08%
		✓	×	R_A	×	80.36%	91.12%	83.33%	76.19%	49.26%	40.20%	70.08%
		✓	R_P	R_A	×	78.64%	88.12%	84.11%	77.21%	52.65%	40.20%	70.16%
✓	R_P	R_A	R_D	81.43%	92.29%	89.71%	78.89%	52.91%	41.40%	72.77%		

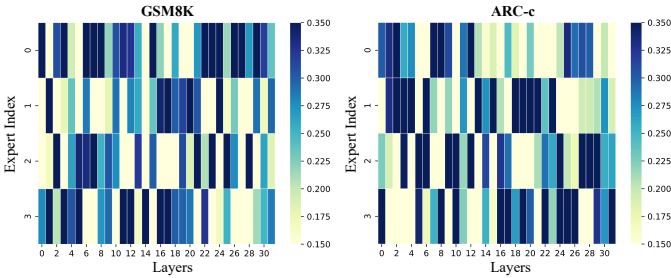


Fig. 7. The activation patterns of experts across layers. The distribution of the routing policy is relatively sparse on both the tasks of GSM8K and ARC-c.

of each expert. Specifically, for each token in a sequence, we only assign “1” to the chosen experts and “0” to the remaining ones. Then, we calculate the proportions of tokens that are routed through each expert, where the number of tokens per expert is normalized over that of all experts. Such a proportion of expert activation reflects the learning preference and the effectiveness of the MoE system. We observe that on both the GSM8K and the ARC-c datasets, the distribution of activation is relatively sparse across layers and each expert is nearly uniformly activated over the entire datasets. Such activation patterns confirm that the MoE system does not collapse equivalently into a single model, where the routing mechanism responds to tokens adaptively and each expert contributes to the overall MoE system.

4.5 Ablation Study on Model Selection

4.5.1 Baselines

In terms of our model selection strategy, four baselines are introduced for comparison: 1) random selection of models from the LoRA Bank (Random), 2) selection of top-ranked models merely by reasoning perplexity (R_P), 3) selection of top-ranked models merely by performance in accuracy (R_A), and 4) selection of top-ranked models by perplexity and performance without considering intra-group diversity (R_D). The selected N experts by each method are used to initialize a MoE system and fine-tuned following the same data augmentation pipeline on $D_K \cup D_A$. For the Random method, we also perform sampling three times for initialization and fine-tuning of three MoE systems. Their averaged results are reported here.

4.5.2 The selection of promising models by comprehensive consideration of performance, reasoning perplexity, and group diversity outperforms the vanilla, simple ones that solely emphasize one aspect

Firstly, we found that the performance of LoRA models randomly selected from the LoRA bank for tasks of interest is incompetent. This suggests that only the most relevant set of models can enhance the performance of specific tasks. As shown in Table 2, our proposed model selection strategy outperforms the approaches that solely rely on K -shot performance and reasoning perplexity. Moreover, using a single model with either the lowest perplexity or the maximized performance for identical initialization of our MoE system (also known as upcycling) results in lower performance. Compared with a group of experts with diversity concerns, the MoE system initialized by the same experts only achieve similar results with Source Best SFT, indicating that highly similar models are detrimental to the training of MoE.

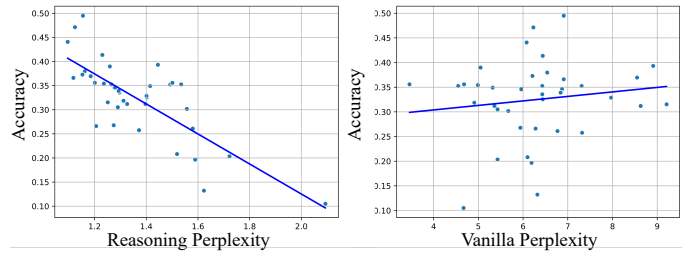


Fig. 8. Comparison between the model selection strategies with the vanilla perplexity on answer choices and the reasoning perplexity on CoT rationales of the ARC-c dataset. A high negative correlation is observed between the performance (exact match accuracy) and the reasoning perplexity. On the contrary, it is difficult to accurately identify promising candidate experts from the vanilla perplexity due to its weak association with performance.

4.5.3 The reasoning perplexity outperforms the vanilla perplexity in model selection

We compared the reasoning perplexity and the vanilla perplexity (without CoT rationales) for model selection. As shown in Fig. 8, with the expanded CoT process, the reasoning perplexity of candidate models has a higher correlation with their performance on testing sets. Consequently, model selection by the reasoning perplexity is more robust than that by the vanilla perplexity.

TABLE 3
Ablation study on the data selection strategy for augmentation in fine-tuning the MoE system.

Model	Method	Similarity	Diversity	ARC-c	ARC-e	BoolQ	PiQA	GSM8K	MBPP	Avg.	
Mistral-7B	<i>K</i> -shot Only	×	×	79.32%	88.67%	79.23%	73.21%	46.67%	40.00%	67.85%	
	Random	×	×	78.42%	84.56%	83.12%	71.21%	48.96%	38.80%	67.51%	
	Ours	Cosine	×	×	82.13%	90.30%	90.01%	75.73%	51.55%	42.40%	72.02%
		Cosine	✓	✓	81.43%	92.29%	89.71%	78.89%	52.91%	41.40%	72.77%
		Convex	✓	✓	82.02%	91.45%	91.43%	79.53%	52.84%	41.40%	73.11%
		KDE ($\gamma=2$)	✓	✓	83.45%	92.34%	88.53%	77.92%	53.43%	41.40%	72.85%
KDE ($\gamma=10$)	✓	✓	80.43%	92.74%	90.55%	79.43%	53.92%	42.00%	73.18%		

4.6 Ablation Study on Data Selection

4.6.1 Baselines

To validate the effectiveness of our data selection strategy, we compare with MoE systems fine-tuned on: 1) *K*-shot data only (*K*-shot Only), 2) randomly selected data from D_S (Random), 3) data selected by cosine similarity without considering diversity, 4) data selected by convex hull with the proposed diversity control, 5) data selected by kernel density estimation (KDE) [19] with the proposed diversity control, 6) data selected by cosine similarity with Repr Filter-based diversity control [55]. All methods were performed on the same initialized MoE system but using different D_A . Except for *K*-shot MoE, we set the data budget C to be the same as 1K for all methods. Due to diversity control, Repr Filter and the proposed method discard duplicates and reduce the size of D_C for a slightly smaller D_A .

To mathematically describe the convex hull-based data selection, we first define the convex hull U_K^C of the given *K*-shot data D_K with their embeddings U_K :

$$U_K^C = \{u | u = \sum_{i=1}^K \lambda_i u_i, u_i \in U_K, \lambda_i \geq 0, \sum_{i=1}^K \lambda_i = 1\}, \quad (16)$$

where λ_i are the coefficients that determine the convex combination of samples in U_K . Then, the convex-hull-based data selection is performed by randomly sampling a subset $D_C \subset D_S, |D_C| = C$ whose embeddings are located inside U_K^C , namely $u_j \in U_K^C, u_j \in U_C$ holds true for $\forall (x_j, y_j) \in D_C$.

The kernel density estimation (KDE) is a non-parametric geometric technique to estimate the probability density function of a random variable. Given the *K*-shot D_K and their embeddings U_K , the estimated density probability of any sample u in the embedding space is presented by:

$$p(u) = \frac{1}{K \cdot \gamma} \sum_{i=1}^K Ker\left(\frac{u - u_i}{\gamma}\right), u_i \in U_K, \quad (17)$$

where $Ker(\cdot)$ denotes the Gaussian kernel function for distance measurement and γ is the bandwidth controlling the smoothness of the density function. For KDE-based data selection, we sample a subset $D_C \subset D_S, |D_C| = C$ according to the probability $p(u_j), u_j \in U_S$. Samples that are closer to *K*-shot data on average are of higher likelihood to be selected.

4.6.2 The open-source data augmentation by similarity-first and diversity-aware selection further improves the MoE system

We investigated the performance of fine-tuning under different data augmentation scenarios. As shown in Table 3, data augmentation based on cosine similarity alone effectively enhances the

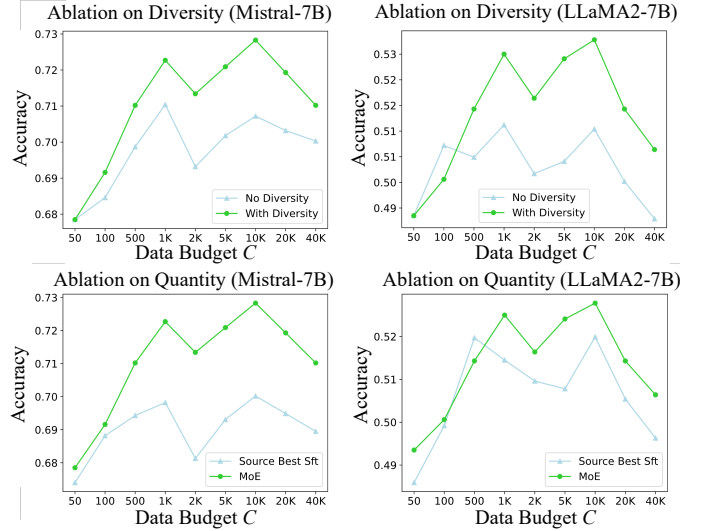


Fig. 9. As the data budget C increases, the performance exhibits a trend of initially rising and then declining. It indicates that the augmentation by truly relevant data improves performance. However, the dominance of irrelevant, redundant samples degrades performance as they dilute the contributions of *K*-shot similar samples. Diversity also plays an important role in balancing distributions, which alleviates overfitting in fine-tuning the MoE system.

performance of our MoE on tasks of interest. However, as shown in Fig. 9, with the increasing amount of data D_A , the performance exhibits a pattern of an initial growth followed by a decline. Such a trend indicates that at the beginning, the involvement of more task-relevant open data exerts an instant positive effect on performance, which not only brings in knowledge but also stabilizes MoE optimization. Accompanied by the enlarged dataset, an excessive amount of irrelevant data begin to dominate. They dilute the contribution of *K*-shot related datapoints and easily cause the system’s forgetting of task-specific skills and knowledge.

Additionally, we examined the role of diversity in data selection. Fig. 9 reveals that filtering out data with high semantic similarity leads to a noticeable improvement in the model’s performance. Especially when the number of data budget C increases, deduplication becomes an indispensable step to mitigate overfitting.

4.6.3 The implementation of similarity-based selection by cosine distance can be replaced with other competitive geometric sampling techniques

Besides, we conducted a comparison between different sampling schemes, including the vanilla selection by minimizing cosine distance (Eq. 13), random sampling within the convex hull enclosed

TABLE 4
Ablation study on the K of K -shot.

Model	Method	ARC-c	ARC-e	BoolQ	PiQA	GSM8K	MBPP	Avg.
LLaMA2-7B	$K = 1$	50.68%	65.08%	62.14%	61.53%	17.29%	20.40%	46.19%
	$K = 5$	57.00%	72.64%	68.41%	64.10%	22.98%	23.80%	51.49%
	$K = 20$	57.49%	73.39%	69.01%	64.82%	24.57%	24.00%	52.20%
	$K = 50$	57.76%	73.60%	69.45%	65.13%	24.83%	24.20%	52.50%
Mistral-7B	$K = 1$	76.27%	89.24%	83.73%	75.77%	45.56%	37.80%	68.06%
	$K = 5$	80.72%	90.98%	89.12%	78.31%	51.92%	40.80%	71.98%
	$K = 20$	81.02%	91.27%	89.53%	78.75%	52.85%	41.20%	72.43%
	$K = 50$	81.43%	92.29%	89.71%	78.89%	52.91%	41.40%	72.77%

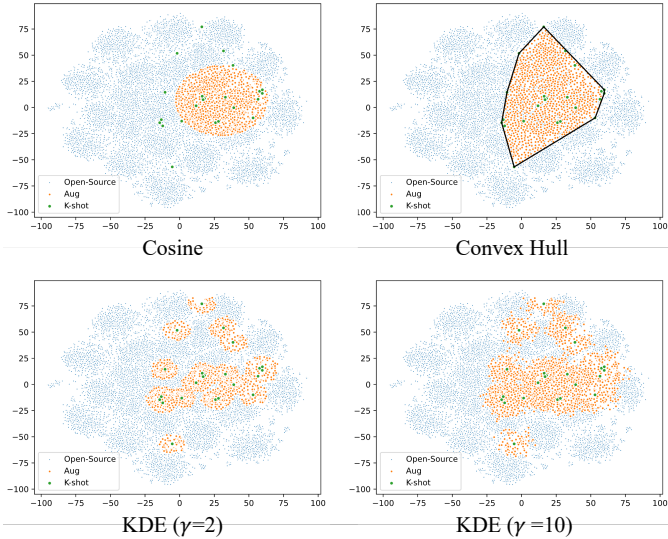


Fig. 10. T-SNE visualization of different similarity-based selection methods including cosine distance, convex hull, and KDE. Blue dots, green dots, and orange dots respectively represent the entire open-source datapoints, the K -shot data, and the selected C samples for augmentation.

by K -shot data (Eq. 16), and sampling based on the estimated density probability (Eq. 17). Given the same budget C , we present a t-SNE [88] visualization of the selected datapoints to highlight the differences between these methods (see Fig. 10).

Table 3 reports that the convex hull-based sampling achieves relatively good results in reasoning tasks such as BoolQ and PiQA. KDE behaves more robustly as it tends to select samples encompassing K -shot as cluster centers. Especially on math and coding tasks, the KDE-based sampling improves the initial MoE the most because it simultaneously introduces samples around K -shot and those extrapolated along boundaries, effectively expanding the knowledge. Furthermore, we notice that the bandwidth γ affects the rate of attenuation in density estimation. A larger γ results in a sparser distribution of the selected data, allowing greater diversity.

4.7 Ablation Study on K , N , and k

4.7.1 The marginal benefits of increasing K on performance decrease

We experimented from $K = 1$ to $K = 50$ (see Table 4) and found that our approach already achieves highly competitive results even under $K = 5$. It demonstrates that the proposed method requires only a small amount of human-verified data to quickly produce expert models with strong professional capabilities. The continual

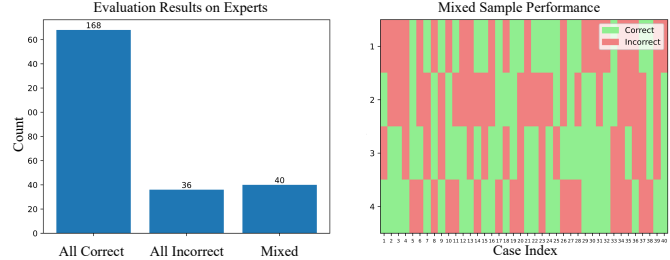


Fig. 11. Evaluation results of each expert (Mistral-7B) in a fine-tuned MoE system on the ARC-c dataset. All Correct and All Incorrect respectively represent the number of cases where all experts succeed and fail. Mixed represents the number of cases where at least one expert perform correctly and at least one incorrectly. For each testing case, correct and incorrect experts are respectively highlighted in green and red.

increase of K from 5 to 50 further improves the performance of the overall MoE system. However, the gains are diminishing, suggesting the trade-off between the efforts of collecting more K -shots and their ultimate profits should be considered.

4.7.2 The dissimilarity between expert candidates is the key to maintaining a task-oriented knowledge-supplementary MoE system

We explored the diversity among expert models for building a successful MoE system. As shown in Fig. 11, we divide the testing cases of the ARC-c into all correct, all incorrect, and mixed, where the constituting experts respectively all succeed, all fail, and perform in between. For all correct cases, all experts are capable of independently solving these cases without external assistance. While for all incorrect cases, case-by-case knowledge injection becomes a requisite to master the missing preliminaries. For the mixed cases, it is the judgement by the routing that resolves disagreement between experts and makes the best use of model ensemble for improvement. Table 5 reports the error rate of each expert and the MoE system on the ARC-c. It can be observed that each expert is adept at different testing cases, exhibiting a varied distribution across experts. Besides, the error rate of the overall MoE system is much lower than that of each expert, confirming the advantages of knowledge expansion. During model selection, the heterogeneity of experts measured by their parameters guarantees the success of a constructed MoE, where the knowledge of each expert supplements to the others.

4.7.3 The amount of data points for fine-tuning the MoE system should be optimized for the task of interest

The amount of data required to effectively train a MoE system, especially the token-wise routing mechanism, remains an intriguing

TABLE 5

Error rates of the MoE system and its four experts (Mistral-7B) on the mixed cases of the ARC-c, where at least one expert succeeds and one expert fails on each sample.

Model	Expert 1	Expert 2	Expert 3	Expert 4	MoE
Error	55.0%	62.5%	37.5%	45.0%	32.5%

question to discuss. In the present study, we utilized a total of 1K data for fine-tuning the MoE system by default. Compared with a single LoRA model, the MoE system yields an increase of +1.05% on LLaMA and +2.95% on Mistral under the same data volume. As confirmed in Fig. 7, the activation of routers is adequately dispersed across layers. It suggests that the optimization of routing weights converges even with 1K data. Moreover, we believe that the quantity of learnable parameters and routing weights in a MoE system should be positively correlated with the volume of data. For larger language models (e.g., 70B and 110B), the data budget C should exceed 1K and potentially reaches up to 10K. In our preliminary experiments, we also find that the complexity of the downstream tasks is worthy of consideration. For simpler tasks such as multiple-choice QA, the appropriate data volume hovers around 0.5K-1K. On the contrary, for challenging tasks such as math and coding problems, 5K-10K data are encouraged. The perplexity of each task by measuring the IFD score [48] of K -shot might be indicative in setting the optimal C .

TABLE 6

Ablation study on the number of experts N . Results on all downstream tasks are averaged.

Model	Number of Experts N			
	2	4	6	8
LLaMA2-7B	52.19%	52.50%	52.43%	50.49%
Mistral-7B	70.45%	72.77%	72.19%	69.84%

4.7.4 *The number of experts does not need to be large for high capacity*

In Table 6, we observe that a small number (e.g., four) of high-quality experts can yield better performance in a MoE system. One reason behind the degraded performance with an increasing number of experts is that the training of a MoE system with numerous experts requires more open-source datasets during optimization. Under the same K -shot settings with data augmentation, the optimization of an eight-expert MoE system is more challenging. It becomes more difficult for the routing itself to converge with fewer data points.

TABLE 7

Ablation study on the number of selected experts k in a 4-expert MoE. Results on all downstream tasks are averaged.

Model	Number of the Selected Experts k			
	1	2	3	4
LLaMA2-7B	49.93%	52.50%	51.19%	52.89%
Mistral-7B	71.82%	72.77%	73.12%	71.64%

4.7.5 *The optimal number of selected experts is not consistent across model architectures*

We initialized the MoE system with four experts, and fine-tuned four MoE models respectively with top-1, top-2, top-3, and all selected experts during routing. Table 7 confirms that when only one expert is selected, the optimization of the MoE system is sub-optimal. With an increase in the number of selected experts k , the performance gradually improves. However, we notice that the optimal number of selected experts is different between the LLaMA and Mistral models. Meticulous efforts on choosing the number of selected experts might be needed to achieve the best performance of the given MoE system.

5 DISCUSSION

5.1 Non-use of Meta Info from the Datasets and Models

In the present study, we do not rely on metadata (e.g., descriptions) to select datasets and models for the following three reasons. First, the descriptions of various open-source models and datasets are often insufficiently detailed. A thorough understanding of the dataset composition or model characteristics demands delving into the semantics of datapoints and the representations of the model layers. Second, each dataset may consist of subsets spanning a wide range of domains and tasks. Identifying the most relevant data points necessitates data selection in the embedding space for retaining only samples that contribute to mastering task-dependent skills. Third, it is challenging to keep track of all the constantly updating metadata on the internet due to privacy and copyrights issues. On the other hand, it is more feasible to only access datasets and models as long as they are available online.

5.2 Applicability and Availability

The proposed comprehensive, scalable pipeline begins with the collection and preparation of datasets and models, followed by the selection of expert candidates and data augmentation for downstream tasks, and culminates at the construction and optimization of a MoE system for the optimized task expertise. Note that a majority of open-source LLMs are variants of the LLaMA and Mistral families that undergo instruction tuning and preference alignment in different ways. A simple search on Huggingface retrieves hundreds of models of the identical size and architecture, profit from the contributions of the open-source community to the development of LLMs. Therefore, the availability of a large model bank is ensured in practical scenarios. It is noted that in the present study, LoRA modules, namely the offsets to the parameters of the base model, are investigated as the main existing forms of model parameters. However, there exist numerous open models that are developed with other PEFT techniques such as adapters. Our approach necessitates the computation of inter-model similarity between weights, which may not be compatible across different PEFT methods. We leave the issue of applicability beyond LoRA modules to be addressed in the future work.

6 CONCLUSION

In this study, we developed an efficient and scalable pipeline to fully utilize K -shot data from downstream tasks of interest for augmentation of existing LLMs in task expertise. The K -shot samples play an important role in both model selection and data augmentation. Specifically, we comprehensively assess the

capability of each expert candidate on K -shot data by simultaneously measuring its performance in exact match accuracy and its reasoning perplexity via auto-regressive language modeling. We bring in diversity by extending the knowledge boundary enclosed by the selected experts, which lays a solid foundation for initializing a flexible MoE system. For optimizing the token-wise collaboration between experts, we propose to fine-tune the MoE with a data augmentation technique. Under such circumstance, a similarity-first, diversity-aware data selection method is developed where the K -shot data steer the selection of task-relevant samples in the embedding space. Diversity is also highlighted by removing the semantic duplicates for alleviating overfitting under data scarce scenarios. Experimental results demonstrate that the proposed method outperforms existing approaches in producing a MoE system of specific task expertise. Extensive ablation studies confirm the validity of the proposed selection methods in pinpointing the most promising models and appropriate data with K -shot, demonstrating a cost-efficient pipeline to excavate open knowledge for customized skill consolidation.

REFERENCES

- [1] Winogrande: An adversarial winograd schema challenge at scale. 2019.
- [2] Amro Abbas, Kushal Tirumala, Dániel Simig, Surya Ganguli, and Ari S Morcos. Semdedup: Data-efficient learning at web-scale through semantic deduplication. *arXiv preprint arXiv:2303.09540*, 2023.
- [3] Josh Achiam, Steven Adler, Sandhini Agarwal, Lama Ahmad, Ilge Akkaya, Florencia Leoni Aleman, Diogo Almeida, Janko Altschmidt, Sam Altman, Shyamal Anadkat, et al. Gpt-4 technical report. *arXiv preprint arXiv:2303.08774*, 2023.
- [4] Shourya Aggarwal, Divyanshu Mandowara, Vishwajeet Agrawal, Dinesh Khandelwal, Parag Singla, and Dinesh Garg. Explanations for commonsenseqa: New dataset and models. In *Proceedings of the 59th Annual Meeting of the Association for Computational Linguistics and the 11th International Joint Conference on Natural Language Processing (Volume 1: Long Papers)*, pages 3050–3065, 2021.
- [5] Aida Amini, Saadia Gabriel, Peter Lin, Rik Koncel-Kedziorski, Yejin Choi, and Hannaneh Hajishirzi. Mathqa: Towards interpretable math word problem solving with operation-based formalisms. *arXiv preprint arXiv:1905.13319*, 2019.
- [6] Jacob Austin, Augustus Odena, Maxwell Nye, Maarten Bosma, Henryk Michalewski, David Dohan, Ellen Jiang, Carrie Cai, Michael Terry, Quoc Le, et al. Program synthesis with large language models. *arXiv preprint arXiv:2108.07732*, 2021.
- [7] Jinze Bai, Shuai Bai, Yunfei Chu, Zeyu Cui, Kai Dang, Xiaodong Deng, Yang Fan, Wenbin Ge, Yu Han, Fei Huang, et al. Qwen technical report. *arXiv preprint arXiv:2309.16609*, 2023.
- [8] Lukas Balles, Giovanni Zappella, and Cédric Archambeau. Gradient-matching coresets for rehearsal-based continual learning. *arXiv preprint arXiv:2203.14544*, 2022.
- [9] Samyadeep Basu, Philip Pope, and Soheil Feizi. Influence functions in deep learning are fragile. *arXiv preprint arXiv:2006.14651*, 2020.
- [10] Joshua Belofsky. Token-level adaptation of lora adapters for downstream task generalization. In *Proceedings of the 2023 6th Artificial Intelligence and Cloud Computing Conference*, pages 168–172, 2023.
- [11] Gantavya Bhatt, Yifang Chen, Arnab M Das, Jifan Zhang, Sang T Truong, Stephen Mussmann, Yinglun Zhu, Jeffrey Bilmes, Simon S Du, Kevin Jamieson, et al. An experimental design framework for label-efficient supervised finetuning of large language models. *arXiv preprint arXiv:2401.06692*, 2024.
- [12] Yonatan Bisk, Rowan Zellers, Jianfeng Gao, Yejin Choi, et al. Piqa: Reasoning about physical commonsense in natural language. In *Proceedings of the AAAI conference on artificial intelligence*, volume 34, pages 7432–7439, 2020.
- [13] Jonathan Brophy, Zayd Hammoudeh, and Daniel Lowd. Adapting and evaluating influence-estimation methods for gradient-boosted decision trees. *Journal of Machine Learning Research*, 24(154):1–48, 2023.
- [14] Oana-Maria Camburu, Tim Rocktäschel, Thomas Lukasiewicz, and Phil Blunsom. e-snli: Natural language inference with natural language explanations. *Advances in Neural Information Processing Systems*, 31, 2018.
- [15] Yihan Cao, Yanbin Kang, Chi Wang, and Lichao Sun. Instruction mining: When data mining meets large language model finetuning. *arXiv preprint arXiv*, 2307, 2023.
- [16] Hao Chen, Yiming Zhang, Qi Zhang, Hantao Yang, Xiaomeng Hu, Xuetao Ma, Yifan Yanggong, and Junbo Zhao. Maybe only 0.5% data is needed: A preliminary exploration of low training data instruction tuning. *arXiv preprint arXiv:2305.09246*, 2023.
- [17] Jianlv Chen, Shitao Xiao, Peitian Zhang, Kun Luo, Defu Lian, and Zheng Liu. Bge m3-embedding: Multi-lingual, multi-functionality, multi-granularity text embeddings through self-knowledge distillation. *arXiv preprint arXiv:2402.03216*, 2024.
- [18] Lichang Chen, Shiyang Li, Jun Yan, Hai Wang, Kalpa Gunaratna, Vikas Yadav, Zheng Tang, Vijay Srinivasan, Tianyi Zhou, Heng Huang, et al. Alpargus: Training a better alpaca with fewer data. *arXiv preprint arXiv:2307.08701*, 2023.
- [19] Yen-Chi Chen. A tutorial on kernel density estimation and recent advances. *Biostatistics & Epidemiology*, 1(1):161–187, 2017.
- [20] Alexandra Chronopoulou, Matthew E Peters, Alexander Fraser, and Jesse Dodge. Adaptersoup: Weight averaging to improve generalization of pretrained language models. *arXiv preprint arXiv:2302.07027*, 2023.
- [21] Christopher Clark, Kenton Lee, Ming-Wei Chang, Tom Kwiatkowski, Michael Collins, and Kristina Toutanova. Boolq: Exploring the surprising difficulty of natural yes/no questions. *arXiv preprint arXiv:1905.10044*, 2019.
- [22] Peter Clark, Isaac Cowhey, Oren Etzioni, Tushar Khot, Ashish Sabharwal, Carissa Schoenick, and Oyvind Tafjord. Think you have solved question answering? try arc, the ai2 reasoning challenge. *arXiv preprint arXiv:1803.05457*, 2018.
- [23] Karl Cobbe, Vineet Kosaraju, Mohammad Bavarian, Mark Chen, Heewoo Jun, Lukasz Kaiser, Matthias Plappert, Jerry Tworek, Jacob Hilton, Reiichiro Nakano, et al. Training verifiers to solve math word problems. *arXiv preprint arXiv:2110.14168*, 2021.
- [24] Alexis Conneau, Kartikay Khandelwal, Naman Goyal, Vishrav Chaudhary, Guillaume Wenzek, Francisco Guzmán, Edouard Grave, Myle Ott, Luke Zettlemoyer, and Veselin Stoyanov. Unsupervised cross-lingual representation learning at scale. *CoRR*, abs/1911.02116, 2019.
- [25] Tim Dettmers, Artidoro Pagnoni, Ari Holtzman, and Luke Zettlemoyer. Qlora: Efficient finetuning of quantized llms. *Advances in Neural Information Processing Systems*, 36, 2024.
- [26] Kaustubh D Dhole, Varun Gangal, Sebastian Gehrmann, Aadesh Gupta, Zhenhao Li, Saad Mahamood, Abinaya Mahendiran, Simon Mille, Ashish Shrivastava, Samson Tan, et al. NI-augmenter: A framework for task-sensitive natural language augmentation. *arXiv preprint arXiv:2112.02721*, 2021.
- [27] Qianlong Du, Chengqing Zong, and Jiajun Zhang. Mods: Model-oriented data selection for instruction tuning. *arXiv preprint arXiv:2311.15653*, 2023.
- [28] Jon Durbin. Airoboros. <https://github.com/jondurbin/airoboros>, 2024.
- [29] Wenfeng Feng, Chuzhan Hao, Yuewei Zhang, Yu Han, and Hao Wang. Mixture-of-loras: An efficient multitask tuning for large language models. *arXiv preprint arXiv:2403.03432*, 2024.
- [30] Mor Geva, Daniel Khashabi, Elad Segal, Tushar Khot, Dan Roth, and Jonathan Berant. Did aristotle use a laptop? a question answering benchmark with implicit reasoning strategies. *Transactions of the Association for Computational Linguistics*, 9:346–361, 2021.
- [31] M Hayes, A Mathur, J Xie, J Wan, S Shah, A Ghodsi, P Wendell, M Zaharia, and R Xin. Free dolly: Introducing the world’s first truly open instruction-tuned llm. 2023.
- [32] Edward J Hu, Yelong Shen, Phillip Wallis, Zeyuan Allen-Zhu, Yuanzhi Li, Shean Wang, Lu Wang, and Weizhu Chen. Lora: Low-rank adaptation of large language models. *arXiv preprint arXiv:2106.09685*, 2021.
- [33] Chengsong Huang, Qian Liu, Bill Yuchen Lin, Tianyu Pang, Chao Du, and Min Lin. Lorahub: Efficient cross-task generalization via dynamic lora composition. *arXiv preprint arXiv:2307.13269*, 2023.
- [34] Gabriel Ilharco, Marco Tulio Ribeiro, Mitchell Wortsman, Suchin Gururangan, Ludwig Schmidt, Hannaneh Hajishirzi, and Ali Farhadi. Editing models with task arithmetic. *arXiv preprint arXiv:2212.04089*, 2022.
- [35] Joel Jang, Seungone Kim, Seonghyeon Ye, Doyoung Kim, Lajanugen Logeswaran, Moontae Lee, Kyungjae Lee, and Minjoon Seo. Exploring the benefits of training expert language models over instruction tuning. In *International Conference on Machine Learning*, pages 14702–14729. PMLR, 2023.
- [36] Albert Q Jiang, Alexandre Sablayrolles, Arthur Mensch, Chris Bamford, Devendra Singh Chaplot, Diego de las Casas, Florian Bressand, Gianna

- Lengyel, Guillaume Lample, Lucile Saulnier, et al. Mistral 7b. *arXiv preprint arXiv:2310.06825*, 2023.
- [37] Xisen Jin, Xiang Ren, Daniel Preotiuc-Pietro, and Pengxiang Cheng. Dataless knowledge fusion by merging weights of language models. *arXiv preprint arXiv:2212.09849*, 2022.
- [38] Junmo Kang, Leonid Karlinsky, Hongyin Luo, Zhen Wang, Jacob Hansen, James Glass, Rameswar Panda, Rogerio Feris, and Alan Ritter. Self-moe: Towards compositional large language models with self-specialized experts. *arXiv preprint arXiv:2406.12034*, 2024.
- [39] Tushar Khot, Peter Clark, Michal Guerquin, Peter Jansen, and Ashish Sabharwal. Qasc: A dataset for question answering via sentence composition. In *Proceedings of the AAAI Conference on Artificial Intelligence*, volume 34, pages 8082–8090, 2020.
- [40] John Kirchenbauer, Garrett Honke, Gowthami Somepalli, Jonas Geiping, Daphne Ippolito, Katherine Lee, Tom Goldstein, and David Andre. Lmd3: Language model data density dependence. *arXiv preprint arXiv:2405.06331*, 2024.
- [41] Aran Komatsuzaki, Joan Puigcerver, James Lee-Thorp, Carlos Riquelme Ruiz, Basil Mustafa, Joshua Ainslie, Yi Tay, Mostafa Dehghani, and Neil Houlsby. Sparse upcycling: Training mixture-of-experts from dense checkpoints. *arXiv preprint arXiv:2212.05055*, 2022.
- [42] Guokun Lai, Qizhe Xie, Hanxiao Liu, Yiming Yang, and Eduard Hovy. Race: Large-scale reading comprehension dataset from examinations. *arXiv preprint arXiv:1704.04683*, 2017.
- [43] Matthew Lamm, Jennimaria Palomaki, Chris Alberti, Daniel Andor, Eunsol Choi, Livio Baldini Soares, and Michael Collins. Qed: A framework and dataset for explanations in question answering. *Transactions of the Association for Computational Linguistics*, 9:790–806, 2021.
- [44] Brian Lester, Rami Al-Rfou, and Noah Constant. The power of scale for parameter-efficient prompt tuning. *arXiv preprint arXiv:2104.08691*, 2021.
- [45] Dengchun Li, Yingzi Ma, Naizheng Wang, Zhiyuan Cheng, Lei Duan, Jie Zuo, Cal Yang, and Mingjie Tang. Mixlora: Enhancing large language models fine-tuning with lora based mixture of experts. *arXiv preprint arXiv:2404.15159*, 2024.
- [46] Guohao Li, Hasan Hammoud, Hani Itani, Dmitrii Khizbullin, and Bernard Ghanem. Camel: Communicative agents for “mind” exploration of large language model society. *Advances in Neural Information Processing Systems*, 36:51991–52008, 2023.
- [47] Margaret Li, Suchin Gururangan, Tim Dettmers, Mike Lewis, Tim Althoff, Noah A Smith, and Luke Zettlemoyer. Branch-train-merge: Embarrassingly parallel training of expert language models. *arXiv preprint arXiv:2208.03306*, 2022.
- [48] Ming Li, Yong Zhang, Zhitao Li, Jiuhai Chen, Lichang Chen, Ning Cheng, Jianzong Wang, Tianyi Zhou, and Jing Xiao. From quantity to quality: Boosting llm performance with self-guided data selection for instruction tuning. *arXiv preprint arXiv:2308.12032*, 2023.
- [49] Xiang Lisa Li and Percy Liang. Prefix-tuning: Optimizing continuous prompts for generation. *arXiv preprint arXiv:2101.00190*, 2021.
- [50] Yunxin Li, Shenyuan Jiang, Baotian Hu, Longyue Wang, Wanqi Zhong, Wenhan Luo, Lin Ma, and Min Zhang. Uni-moe: Scaling unified multi-modal llms with mixture of experts. *arXiv preprint arXiv:2405.11273*, 2024.
- [51] Wang Ling, Dani Yogatama, Chris Dyer, and Phil Blunsom. Program induction by rationale generation: Learning to solve and explain algebraic word problems. *arXiv preprint arXiv:1705.04146*, 2017.
- [52] Jerry Liu. LlamaIndex, 11 2022.
- [53] Qidong Liu, Xian Wu, Xiangyu Zhao, Yuanshao Zhu, Derong Xu, Feng Tian, and Yefeng Zheng. Moelora: An moe-based parameter efficient fine-tuning method for multi-task medical applications. *arXiv preprint arXiv:2310.18339*, 2023.
- [54] Shih-Yang Liu, Chien-Yi Wang, Hongxu Yin, Pavlo Molchanov, Yu-Chiang Frank Wang, Kwang-Ting Cheng, and Min-Hung Chen. Dora: Weight-decomposed low-rank adaptation. *arXiv preprint arXiv:2402.09353*, 2024.
- [55] Wei Liu, Weihao Zeng, Keqing He, Yong Jiang, and Junxian He. What makes good data for alignment? a comprehensive study of automatic data selection in instruction tuning. In *The Twelfth International Conference on Learning Representations*, 2024.
- [56] Zefang Liu and Jiahua Luo. Adamole: Fine-tuning large language models with adaptive mixture of low-rank adaptation experts. *arXiv preprint arXiv:2405.00361*, 2024.
- [57] Shayne Longpre, Le Hou, Tu Vu, Albert Webson, Hyung Won Chung, Yi Tay, Denny Zhou, Quoc V Le, Barret Zoph, Jason Wei, et al. The flan collection: Designing data and methods for effective instruction tuning. In *International Conference on Machine Learning*, pages 22631–22648. PMLR, 2023.
- [58] Keming Lu, Hongyi Yuan, Runji Lin, Junyang Lin, Zheng Yuan, Chang Zhou, and Jingren Zhou. Routing to the expert: Efficient reward-guided ensemble of large language models. *arXiv preprint arXiv:2311.08692*, 2023.
- [59] Max Marion, Ahmet Üstün, Luiza Pozzobon, Alex Wang, Marzieh Fadaee, and Sara Hooker. When less is more: Investigating data pruning for pretraining llms at scale. *arXiv preprint arXiv:2309.04564*, 2023.
- [60] Fanxu Meng, Zhaohui Wang, and Muhan Zhang. Pissa: Principal singular values and singular vectors adaptation of large language models. *arXiv preprint arXiv:2404.02948*, 2024.
- [61] Microsoft. Wizardlm-2 8x22b, 2024.
- [62] Subhabrata Mukherjee, Arindam Mitra, Ganesh Jawahar, Sahaj Agarwal, Hamid Palangi, and Ahmed Awadallah. Orca: Progressive learning from complex explanation traces of gpt-4. *arXiv preprint arXiv:2306.02707*, 2023.
- [63] Mohammed Muqeeth, Haokun Liu, Yufan Liu, and Colin Raffel. Learning to route among specialized experts for zero-shot generalization. *arXiv preprint arXiv:2402.05859*, 2024.
- [64] Mohammed Muqeeth, Haokun Liu, and Colin Raffel. Soft merging of experts with adaptive routing. *arXiv preprint arXiv:2306.03745*, 2023.
- [65] Reiichiro Nakano, Jacob Hilton, Suchir Balaji, Jeff Wu, Long Ouyang, Christina Kim, Christopher Hesse, Shantanu Jain, Vineet Kosaraju, William Saunders, et al. Webgpt: Browser-assisted question-answering with human feedback. *arXiv preprint arXiv:2112.09332*, 2021.
- [66] Yasumasa Onoe, Michael JQ Zhang, Eunsol Choi, and Greg Durrett. Creak: A dataset for commonsense reasoning over entity knowledge. *arXiv preprint arXiv:2109.01653*, 2021.
- [67] Oleksiy Ostapenko, Zhan Su, Edoardo Maria Ponti, Laurent Charlin, Nicolas Le Roux, Matheus Pereira, Lucas Caccia, and Alessandro Sordoni. Towards modular llms by building and reusing a library of lorae. *arXiv preprint arXiv:2405.11157*, 2024.
- [68] Simon Ott, Konstantin Hebenstreit, Valentin Liévin, Christoffer Egeberg Hother, Milad Moradi, Maximilian Mayrhauser, Robert Praas, Ole Winther, and Matthias Samwald. Thoughtsource: A central hub for large language model reasoning data. *Scientific Data*, 10(1):528, 2023.
- [69] Lucas Page-Caccia, Edoardo Maria Ponti, Zhan Su, Matheus Pereira, Nicolas Le Roux, and Alessandro Sordoni. Multi-head adapter routing for cross-task generalization. *Advances in Neural Information Processing Systems*, 36, 2024.
- [70] Adam Paszke, Sam Gross, Francisco Massa, Adam Lerer, James Bradbury, Gregory Chanan, Trevor Killeen, Zeming Lin, Natalia Gimelshein, Luca Antiga, et al. Pytorch: An imperative style, high-performance deep learning library. *Advances in neural information processing systems*, 32, 2019.
- [71] Baolin Peng, Chunyuan Li, Pengcheng He, Michel Galley, and Jianfeng Gao. Instruction tuning with gpt-4. *arXiv preprint arXiv:2304.03277*, 2023.
- [72] Jonas Pfeiffer, Andreas Rücklé, Clifton Poth, Aishwarya Kamath, Ivan Vulić, Sebastian Ruder, Kyunghyun Cho, and Iryna Gurevych. Adapterhub: A framework for adapting transformers. *arXiv preprint arXiv:2007.07779*, 2020.
- [73] Agustin Picard, Lucas Hervier, Thomas Fel, and David Vigouroux. Influence: A library for tracing the influence back to the data-points. In *World Conference on Explainable Artificial Intelligence*, pages 193–204. Springer, 2024.
- [74] Yulei Qin, Yuncheng Yang, Pengcheng Guo, Gang Li, Hang Shao, Yuchen Shi, Zihan Xu, Yun Gu, Ke Li, and Xing Sun. Unleashing the power of data tsunami: A comprehensive survey on data assessment and selection for instruction tuning of language models. 2024.
- [75] Zheng Lin Qingyi Si. Alpaca-cot: An instruction fine-tuning platform with instruction data collection and unified large language models interface. <https://github.com/PhoebusSi/alpaca-CoT>, 2023.
- [76] Jeff Rasley, Samyam Rajbhandari, Olatunji Ruwase, and Yuxiong He. DeepSpeed: System optimizations enable training deep learning models with over 100 billion parameters. In *Proceedings of the 26th ACM SIGKDD International Conference on Knowledge Discovery & Data Mining*, pages 3505–3506, 2020.
- [77] Maarten Sap, Hannah Rashkin, Derek Chen, Ronan LeBras, and Yejin Choi. Socialliqa: Commonsense reasoning about social interactions. *arXiv preprint arXiv:1904.09728*, 2019.
- [78] Timo Schick, Jane Dwivedi-Yu, Roberto Dessì, Roberta Raileanu, Maria Lomeli, Eric Hambro, Luke Zettlemoyer, Nicola Cancedda, and Thomas Scialom. Toolformer: Language models can teach themselves to use tools. *Advances in Neural Information Processing Systems*, 36, 2024.

- [79] Stephanie Schoch, Ritwick Mishra, and Yangfeng Ji. Data selection for fine-tuning large language models using transferred shapley values. *arXiv preprint arXiv:2306.10165*, 2023.
- [80] Ozan Sener and Silvio Savarese. Active learning for convolutional neural networks: A core-set approach. *arXiv preprint arXiv:1708.00489*, 2017.
- [81] Rico Sennrich, Barry Haddow, and Alexandra Birch. Improving neural machine translation models with monolingual data. *arXiv preprint arXiv:1511.06709*, 2015.
- [82] Samarth Sinha, Han Zhang, Anirudh Goyal, Yoshua Bengio, Hugo Larochelle, and Augustus Odena. Small-gan: Speeding up gan training using core-sets. In *International Conference on Machine Learning*, pages 9005–9015. PMLR, 2020.
- [83] Zhan Su, Fengran Mo, Prayag Tiwari, Benyou Wang, Jian-Yun Nie, and Jakob Grue Simonsen. Mixture of experts using tensor products. *arXiv preprint arXiv:2405.16671*, 2024.
- [84] Sainbayar Sukhbaatar, Olga Golovneva, Vasu Sharma, Hu Xu, Xi Victoria Lin, Baptiste Rozière, Jacob Kahn, Daniel Li, Wen-tau Yih, Jason Weston, et al. Branch-train-mix: Mixing expert llms into a mixture-of-experts llm. *arXiv preprint arXiv:2403.07816*, 2024.
- [85] Alon Talmor, Jonathan Herzig, Nicholas Lourie, and Jonathan Berant. Commonsenseqa: A question answering challenge targeting common-sense knowledge. *arXiv preprint arXiv:1811.00937*, 2018.
- [86] Kushal Tirumala, Daniel Simig, Armen Aghajanyan, and Ari Morcos. D4: Improving llm pretraining via document de-duplication and diversification. *Advances in Neural Information Processing Systems*, 36, 2024.
- [87] Hugo Touvron, Louis Martin, Kevin Stone, Peter Albert, Amjad Almahairi, Yasmine Babaei, Nikolay Bashlykov, Soumya Batra, Prajjwal Bhargava, Shruti Bhosale, et al. Llama 2: Open foundation and fine-tuned chat models. *arXiv preprint arXiv:2307.09288*, 2023.
- [88] Laurens Van der Maaten and Geoffrey Hinton. Visualizing data using t-sne. *Journal of machine learning research*, 9(11), 2008.
- [89] Cunxiang Wang, Shuailong Liang, Yue Zhang, Xiaonan Li, and Tian Gao. Does it make sense? and why? a pilot study for sense making and explanation. *arXiv preprint arXiv:1906.00363*, 2019.
- [90] Eric J. Wang. Alpaca-lora. <https://github.com/tloen/alpaca-lora>, 2024.
- [91] Yizhong Wang, Yeganeh Kordi, Swaroop Mishra, Alisa Liu, Noah A Smith, Daniel Khashabi, and Hannaneh Hajishirzi. Self-instruct: Aligning language models with self-generated instructions. *arXiv preprint arXiv:2212.10560*, 2022.
- [92] Zengzhi Wang, Rui Xia, and Pengfei Liu. Generative ai for math: Part i—mathpile: A billion-token-scale pretraining corpus for math. *arXiv preprint arXiv:2312.17120*, 2023.
- [93] Jason Wei, Xuezhi Wang, Dale Schuurmans, Maarten Bosma, Fei Xia, Ed Chi, Quoc V Le, Denny Zhou, et al. Chain-of-thought prompting elicits reasoning in large language models. *Advances in neural information processing systems*, 35:24824–24837, 2022.
- [94] Jason Wei and Kai Zou. Eda: Easy data augmentation techniques for boosting performance on text classification tasks. *arXiv preprint arXiv:1901.11196*, 2019.
- [95] Thomas Wolf, Lysandre Debut, Victor Sanh, Julien Chaumond, Clement Delangue, Anthony Moi, Pierric Cistac, Tim Rault, Rémi Louf, Morgan Funtowicz, et al. Huggingface’s transformers: State-of-the-art natural language processing. *arXiv preprint arXiv:1910.03771*, 2019.
- [96] Shengguang Wu, Keming Lu, Benfeng Xu, Junyang Lin, Qi Su, and Chang Zhou. Self-evolved diverse data sampling for efficient instruction tuning. *arXiv preprint arXiv:2311.08182*, 2023.
- [97] Xun Wu, Shaohan Huang, and Furu Wei. Mole: Mixture of lora experts. In *The Twelfth International Conference on Learning Representations*, 2023.
- [98] Mengzhou Xia, Sadhika Malladi, Suchin Gururangan, Sanjeev Arora, and Danqi Chen. Less: Selecting influential data for targeted instruction tuning. *arXiv preprint arXiv:2402.04333*, 2024.
- [99] Sang Michael Xie, Shibani Santurkar, Tengyu Ma, and Percy S Liang. Data selection for language models via importance resampling. *Advances in Neural Information Processing Systems*, 36:34201–34227, 2023.
- [100] Can Xu, Qingfeng Sun, Kai Zheng, Xiubo Geng, Pu Zhao, Jiazhan Feng, Chongyang Tao, and Daxin Jiang. Wizardlm: Empowering large language models to follow complex instructions. *arXiv preprint arXiv:2304.12244*, 2023.
- [101] Yang Xu, Yongqiang Yao, Yufan Huang, Mengnan Qi, Maoquan Wang, Bin Gu, and Neel Sundaresan. Rethinking the instruction quality: Lift is what you need. *arXiv preprint arXiv:2312.11508*, 2023.
- [102] Prateek Yadav, Derek Tam, Leshem Choshen, Colin A Raffel, and Mohit Bansal. Ties-merging: Resolving interference when merging models. *Advances in Neural Information Processing Systems*, 36, 2024.
- [103] Rui Yang, Lin Song, Yanwei Li, Sijie Zhao, Yixiao Ge, Xiu Li, and Ying Shan. Gpt4tools: Teaching large language model to use tools via self-instruction. *Advances in Neural Information Processing Systems*, 36, 2024.
- [104] Yuncheng Yang, Meng Wei, Junjun He, Jie Yang, Jin Ye, and Yun Gu. Pick the best pre-trained model: Towards transferability estimation for medical image segmentation. In *International Conference on Medical Image Computing and Computer-Assisted Intervention*, pages 674–683. Springer, 2023.
- [105] Kaichao You, Yong Liu, Ziyang Zhang, Jianmin Wang, Michael I Jordan, and Mingsheng Long. Ranking and tuning pre-trained models: a new paradigm for exploiting model hubs. *Journal of Machine Learning Research*, 23(209):1–47, 2022.
- [106] Le Yu, Bowen Yu, Haiyang Yu, Fei Huang, and Yongbin Li. Language models are super mario: Absorbing abilities from homologous models as a free lunch. *arXiv preprint arXiv:2311.03099*, 2023.
- [107] Rowan Zellers, Ari Holtzman, Yonatan Bisk, Ali Farhadi, and Yejin Choi. Hellaswag: Can a machine really finish your sentence? *arXiv preprint arXiv:1905.07830*, 2019.
- [108] Jinghan Zhang, Junteng Liu, Junxian He, et al. Composing parameter-efficient modules with arithmetic operation. *Advances in Neural Information Processing Systems*, 36:12589–12610, 2023.
- [109] Jipeng Zhang, Yaxuan Qin, Renjie Pi, Weizhong Zhang, Rui Pan, and Tong Zhang. Tagcos: Task-agnostic gradient clustered coreset selection for instruction tuning data. *arXiv preprint arXiv:2407.15235*, 2024.
- [110] Qingru Zhang, Minshuo Chen, Alexander Bukharin, Pengcheng He, Yu Cheng, Weizhu Chen, and Tuo Zhao. Adaptive budget allocation for parameter-efficient fine-tuning. In *The Eleventh International Conference on Learning Representations*, 2023.
- [111] Shengyu Zhang, Linfeng Dong, Xiaoya Li, Sen Zhang, Xiaofei Sun, Shuhe Wang, Jiwei Li, Runyi Hu, Tianwei Zhang, Fei Wu, et al. Instruction tuning for large language models: A survey. *arXiv preprint arXiv:2308.10792*, 2023.
- [112] Xiang Zhang, Junbo Zhao, and Yann LeCun. Character-level convolutional networks for text classification. *Advances in neural information processing systems*, 28, 2015.
- [113] Bo Zhao and Hakan Bilen. Dataset condensation with distribution matching. In *Proceedings of the IEEE/CVF Winter Conference on Applications of Computer Vision*, pages 6514–6523, 2023.
- [114] Ziyu Zhao, Leilei Gan, Guoyin Wang, Yuwei Hu, Tao Shen, Hongxia Yang, Kun Kuang, and Fei Wu. Retrieval-augmented mixture of lora experts for uploadable machine learning. *arXiv preprint arXiv:2406.16989*, 2024.
- [115] Chunting Zhou, Pengfei Liu, Puxin Xu, Srinivasan Iyer, Jiao Sun, Yuning Mao, Xuezhe Ma, Avia Efrat, Ping Yu, Lili Yu, et al. Lima: Less is more for alignment. *Advances in Neural Information Processing Systems*, 36, 2024.
- [116] Daquan Zhou, Kai Wang, Jianyang Gu, Xiangyu Peng, Dongze Lian, Yifan Zhang, Yang You, and Jiashi Feng. Dataset quantization. In *Proceedings of the IEEE/CVF International Conference on Computer Vision*, pages 17205–17216, 2023.
- [117] Han Zhou, Xingchen Wan, Ivan Vulić, and Anna Korhonen. Autoteft: Automatic configuration search for parameter-efficient fine-tuning. *Transactions of the Association for Computational Linguistics*, 12:525–542, 2024.
- [118] Kaiyang Zhou, Jingkang Yang, Chen Change Loy, and Zifei Liu. Conditional prompt learning for vision-language models. In *Proceedings of the IEEE/CVF conference on computer vision and pattern recognition*, pages 16816–16825, 2022.

APPENDIX

.1 Datasets

We present the statistics of publicly available datasets used in the present study for constructing our LoRA bank in Table 8.

.2 Evaluation Results of Models in the Bank

The evaluation results of LoRA models in the bank are reported in Tables 9 and 10 respectively for LLaMA2 [87] and Mistral [36] families.

Each model is fine-tuned on one high-quality open dataset under the same experimental settings. Results confirm that all these LoRA models exhibit different advantages on the downstream tasks of interest, implying that each model possesses a unique skill acquired from the fine-tuned dataset. However, we also observe that certain models are highly competitive nearly on all tasks (e.g., RACE for the LLaMA2 and ARC-e for the Mistral). Such phenomenon may be ascribed to the fact that these two datasets emphasize the reasoning and reading comprehension capabilities of LLMs, where the acquired skills appear more general in solving various tasks. Besides, we notice that the two model families (LLaMA vs. Mistral) behave inconsistently in the evaluation results even under the same fine-tuning settings. It suggests that different pre-training corpus are collected and memorized for language modeling, and thereafter the two base pre-trained models already differ in the parameterized knowledge before instruction fine-tuning. Consequently, when optimizing any LLM for the task-of-interest, there exists no golden rule of selecting one generally-applicable, ultimately-superior instruction dataset which would work all the time. In practice, one should dynamically select potential models following the proposed pipeline instead of empirically sampling from the bank. Last but not least, it is noted that the diversity of the candidate models in the bank has to be guaranteed to ensure that each model owns knowledge that can supplement to the other one. Such bank diversity allows a generalized skill-set to be utilized via the constructed MoE system for solving tasks of interest.

.3 Mathematical Notations

In this section, we present the description of all math notations in the manuscript (see Table 11).

.4 Implementation Details

The detailed settings of all hyper-parameters for optimization of the LoRA models and the MoE system are listed in Table 12.

TABLE 8
Statistics of Datasets (Part 1).

Dataset	Task	Train	Val	Test	Example
ARC-c	Exam	1.1K	299	1.1K	{ "instruction": "Question: George wants to warm his hands quickly by rubbing them. Which skin surface will produce the most heat? A. dry palms\nB. wet palms\nC. palms covered with oil\nD. palms covered with lotion\nAnswer:", "input": "", "output": "A. dry palms" }
ARC-c CoT-formatted	Exam	1.1K	299	1.1K	{ "instruction": "Question: George wants to warm his hands quickly by rubbing them. Which skin surface will produce the most heat? A. dry palms\nB. wet palms\nC. palms covered with oil\nD. palms covered with lotion\nAnswer:", "input": "", "output": "Rubbing two surfaces together generates heat due to friction. In the case of warming hands, the effectiveness of this process depends on the coefficient of friction between the surfaces. Dry palms are likely to produce the most heat when rubbed together because they have a higher coefficient of friction compared to wet palms, which would slip more easily and thus generate less heat. Palms covered with oil or lotion would also have reduced friction due to the lubricating effect of these substances, leading to less heat generation upon rubbing. Therefore, dry palms are the most effective choice for generating heat through friction. The answer is A. dry palms" }
ARC-e	Exam	2.2K	570	2.3K	{ "instruction": "Question: Which factor will most likely cause a person to develop a fever? A. a leg muscle relaxing after exercise\nB. a bacterial population in the bloodstream\nC. several viral particles on the skin\nD. carbohydrates being digested in the stomach\nAnswer:", "input": "", "output": "B. a bacterial population in the bloodstream" }
WinoGrande	Coreference Resolution	9.2K	1267	-	{ "instruction": "Which of the following is a good sentence:\nA. John moved the couch from the garage to the backyard to create space. The garage is small.\nB. John moved the couch from the garage to the backyard to create space. The backyard is small.\nAnswer:", "input": "", "output": "A. John moved the couch from the garage to the backyard to create space. The garage is small." }
GSM8K	Math	7.4K	0	1.3K	{ "instruction": "Question: Natalia sold clips to 48 of her friends in April, and then she sold half as many clips in May. How many clips did Natalia sell altogether in April and May?", "input": "", "output": "Answer: Natalia sold $48/2 = 24$ clips in May.\nNatalia sold $48+24 = 72$ clips altogether in April and May." }
PIQA	Commonsense Reasoning	16.1K	1838	3K	{ "instruction": "Question: When boiling butter, when it's ready, you can\nA. Pour it onto a plate\nB. Pour it into a jar\nAnswer:", "input": "", "output": "B. Pour it into a jar" }
CommonSense QA	Commonsense Reasoning	9.7K	1221	1.1K	{ "instruction": "Who is likely to use a comb?A.medicine cabinet\nB.trashcan\nC.suitcase\nD.pocket\nE.barber shop", "input": "", "output": "E.barber shop" }
RACE	Reading Comprehension	87.8K	4887	4.9K	{ "instruction": "Mrs Green lives in a small village. Her husband is dead, but she has one son. His name is Jack. He is twenty-one. He worked in a shop in the village and lived with his mother, but then he finds a job in a faraway town named Green Sea. He goes and lives there. Mrs Green is not happy about it.\nOne day Mrs Green is angry. She gets on a train and goes to her son's house in Green Sea. Then she says to him. \"Jack, why do you never telephone me?\"\nJack smiles, \"But, Mother, you don't have a telephone.\"\n\"No,\" she answers, \"I don't have, but you have one!\"\nGreen Sea is _ the small village.A.in\nB.next to\nC.near\nD.far from", "input": "", "output": "D.far from" }
MBPP	Coding	374	90	500	{ "instruction": "Write a python function to find the first repeated character in a given string.", "input": "", "output": "def first_repeated_char(str1):\r\n for index,c in enumerate(str1):\r\n if str1[index+1].count(c) >1:\r\n return c\r\n return \"None\" }

TABLE 8
Statistics of Datasets (Part 3).

Dataset	Task	Train	Val	Test	Example
QED	CoT	5.1K	–	–	{“instruction”: “Answer the following Q with stream of consciousness. Passage: Webbed toes is the common name for syndactyly affecting the feet. It is characterised by the fusion of two or more digits of the feet. This is normal in many birds, such as ducks; amphibians, such as frogs; and mammals, such as kangaroos. In humans it is considered unusual, occurring in approximately one in 2,000 to 2,500 live births.”\n\nQuestion: “Based on this passage, what is the medical term for webbed toes?”, “input”: “”, “output”: “The relevant information is: Webbed toes is the common name for syndactyly affecting the feet. Therefore, the final answer is syndactyly affecting the feet.”}
StrategyQA	CoT	2K	–	–	{“instruction”: “Answer the following question by reasoning step-by-step. Are more people today related to Genghis Khan than Julius Caesar?”, “input”: “”, “output”: “Julius Caesar had three children. Genghis Khan had sixteen children. Modern geneticists have determined that out of every 200 men today has DNA that can be traced to Genghis Khan. Therefore, the final answer is yes.”}
SensemakingQA	CoT	6K	–	–	{“instruction”: “Of the following two sentences, which one is against common sense?”\nOptions:\n- Sentence A: “He poured orange juice on his cereal.”\n- Sentence B: “He poured milk on his cereal.”\nLet’s be accurate as possible. So think first.”, “input”: “”, “output”: “Orange juice does not taste good on cereal.\n\nThe final answer: Sentence A.”}, {“instruction”: “Let’s think step by step! Which of the following two sentences does not make sense?”\nOptions:\n- Sentence A: “He drinks apple.”\n- Sentence B: “He drinks milk.”\n”, “input”: “”, “output”: “An apple is a whole food and unable to be drunk without being juiced. The answer: Sentence A.”}
Toolformer (th=0.6)	ToolUse	2.4K	–	–	{“instruction”: “toolformer: enabled\n\n toolformer access: wikipedia\n\n a wrapper around Wikipedia. Useful for when you need to display general information about people, places, companies, historical events, or other subjects found in an encyclopedia, displays a snippet summary of the topic. Input should be a search query.\nwikipedia(query)\n\n Provide a summary of a famous historical event based on the input event given”, “input”: “French Revolution”, “output”: “Summary of the French Revolution: wikipedia(‘French Revolution’)”}
HellaSwag	Commonsense Reasoning	39.9K	–	10K	{“instruction”: “[header] How to reset a vizio remote [title] Remove your remote’s batteries. [step] They’re typically found in a slot that’s either on the bottom or in the back of the remote. [title] Press and hold the remote’s power button.\n\n Question: Which ending makes the most sense?A. [step] This allows the device to power off. [title] Press and hold the power button on the remote while you wait to hear a response.B. [step] It’s located near the bottom of the remote, right in the. [title] Release the power button when you’re sure it’s covered.C. [step] It’s usually at the top of the remote’s surface. [title] Release the power button after five seconds.D. [step] Hold down the power button as close to the batteries as possible. This will power up your device and allow the lower battery to refill with power.”, “input”: “”, “output”: “C. [step] It’s usually at the top of the remote’s surface. [title] Release the power button after five seconds.”}
SiQA	Commonsense Reasoning	33.4K	–	1.9K	{“instruction”: “Addison put Kendall’s cost-cutting ideas into action.\n\n What will happen to Addison?\nA. kendall will be thanked\nB. get promoted\nC. lose their job”, “input”: “”, “output”: “B. get promoted”}
BoolQ	Knowledge Question Answering	2.4K	277	3K	{“instruction”: “Good Samaritan laws offer legal protection to people who give reasonable assistance to those who are, or who they believe to be, injured, ill, in peril, or otherwise incapacitated. The protection is intended to reduce bystanders’ hesitation to assist, for fear of being sued or prosecuted for unintentional injury or wrongful death. An example of such a law in common-law areas of Canada: a good Samaritan doctrine is a legal principle that prevents a rescuer who has voluntarily helped a victim in distress from being successfully sued for wrongdoing. Its purpose is to keep people from being reluctant to help a stranger in need for fear of legal repercussions should they make some mistake in treatment. By contrast, a duty to rescue law requires people to offer assistance and holds those who fail to do so liable.\n\n Question: do good samaritan laws protect those who help at an accident\nA. Yes\nB. No\n\n Answer:”, “input”: “”, “output”: “A. Yes”}

TABLE 8
Statistics of Datasets (Part 4).

Dataset	Task	Train	Val	Test	Example
Dolly	CoT	15K	–	–	{ <code>"instruction": "Which American president spoke Dutch as their first language?"</code> ; <code>"input": "Van Buren received a basic education at the village schoolhouse, and briefly studied Latin at the Kinderhook Academy and at Washington Seminary in Claverack. Van Buren was raised speaking primarily Dutch and learned English while attending school; he is the only president of the United States whose first language was not English. Also during his childhood, Van Buren learned at his father's inn how to interact with people from varied ethnic, income, and societal groups, which he used to his advantage as a political organizer. His formal education ended in 1796, when he began reading law at the office of Peter Silvester and his son Francis."</code> ; <code>"output": "President Van Buren spoke Dutch as his first language. He is the only president of the United States of America who spoke English as a second language."}</code> }
WizardLM	General	143K	–	–	{ <code>"instruction": "As an online platform teacher named Aimee, you possess impeccable credentials which include a Bachelor of Science degree in Industrial and Labor Relations from Cornell University, expertise in the English language, and intermediate proficiency in both Chinese and Spanish. Additionally, your professional experience as a STEAM teacher at UN Women in Singapore has honed your skills in teaching children from the ages of 6-11 and working with students from all levels of education. Your exceptional teaching abilities in spoken English and pronunciation paired with your personal strengths of being informed, patient, and engaging make you an ideal teacher for students seeking to improve their English language skills. Can you provide a short, concise, and unique English self-introduction in bullet point form that would attract students to enroll in your course?"</code> ; <code>"output": "Sure, here are some bullet points for your English self-introduction:\n\n Hi there! My name is Aimee and I'm thrilled to be your online English teacher!\n\n With a Bachelor's degree from Cornell University and experience teaching STEAM at UN Women in Singapore, I know how to help students learn effectively.\n\n I'm passionate about language and have intermediate proficiency in both Chinese and Spanish, so I understand the challenges of learning a new language.\n\n In my classes, I focus on improving spoken English and pronunciation, as well as building vocabulary and grammar skills.\n\n But learning English doesn't have to be boring! I'm an engaging and patient teacher who loves to have fun and make learning enjoyable.\n\n So, whether you're a beginner or an advanced student, I'm confident that I can help you improve your English skills and achieve your goals. Let's get started!"</code> ; <code>"input": ""}</code> }
ShareGPT	General	330K	–	–	{ <code>"instruction": "Summarize the main ideas of Jeff Walker's Product Launch Formula into bullet points as it pertains to a growth marketing agency implementing these strategies and tactics for their clients..."</code> ; <code>"input": ""</code> ; <code>"output": "Here are the main ideas of Jeff Walker's Product Launch Formula that can be applied by a growth marketing agency for their clients:\n\n1. Identify the target audience and their needs: Understand the ideal customer for the product or service, and create a messaging that resonates with them.\n\n2. Pre-launch: Build anticipation and excitement for the launch by creating buzz, gathering testimonials and case studies, and using social media to create awareness.\n\n3. Launch: Use a well-crafted launch sequence to maximize sales and conversions. This can include offering bonuses, creating scarcity, and using a deadline to create urgency.\n\n4. Post-launch: Follow up with customers, gather feedback, and continue to provide value to keep them engaged and loyal.\n\n5. Create a product suite: Once the initial product is successful, expand the offering by creating additional products or services that address other needs of the same audience.\n\n6. Continual optimization: Continually monitor and optimize the launch process and product suite to improve results.\n\n7. Build a community: Use the launch process to build a community of customers who are passionate about the product and can help spread the word.\n\n8. Use automation: Use technology and automation to streamline the launch process and improve efficiency."}</code> }
GPT-Teacher-Code	Coding	4.5K	–	–	{ <code>"instruction": "Design a C++ function to calculate the factorial of a non-negative integer."</code> ; <code>"input": "5"</code> ; <code>"output": "#include <iostream>\n\nunsigned long long factorial(int n) {\n if (n <= 1) {\n return 1;\n }\n return n * factorial(n - 1);\n}\n\nint main() {\n int num = 5;\n std::cout <<'Factorial of ' <<num <<' is ' <<factorial(num) <<std::endl;\n return 0;\n}"}</code> }

TABLE 8
Statistics of Datasets (Part 5).

Dataset	Task	Train	Val	Test	Example
GPT-Teacher-Roleplay	Coding	3.1K	-	-	{ <code>"instruction": "Imagine you are a detective trying to solve a murder mystery in a fictional Victorian-era town. Describe the scene of the crime, the main suspects, and your plan to investigate the case."</code> , <code>"input": ""</code> , <code>"output": "The scene of the crime is a dimly lit study inside a grand, Victorian-era mansion. There's a large oak desk at the center of the room, and the deceased, Lord Barrington, lies slumped over it with a gunshot wound to the chest. A shattered windowpane hints at the possible point of entry for the assailant. The three main suspects are: 1) Lady Barrington, the victim's wife, who had increasing disputes with her husband; 2) Randall, the family's loyal butler, who recently discovered he was going to be replaced; and 3) Edgar, a distant cousin, who expected a large inheritance if Lord Barrington passed away. My plan to investigate the case includes: interviewing each suspect about their whereabouts during the crime; examining the broken window for any fingerprints or signs of forced entry; and analyzing the murder weapon, a pistol, to trace its ownership and look for any additional evidence like partial fingerprints or other traces left by the culprit."}</code> }
GPT-Teacher-Instruct	General	17K	-	-	{ <code>"instruction": "Provide an overview of the process of human evolution."</code> , <code>"input": ""</code> , <code>"output": "Human evolution began millions of years ago with the emergence of common ancestors of humans, chimpanzees, and gorillas. The process involved a series of distinct species branching off and evolving separately, with some leading to modern humans, Homo sapiens. Key milestones in human evolution include the appearance of the first hominids (human-like primates), the development of bipedalism (walking upright), and the growth of larger brains. Over time, hominids developed more advanced tools, communication abilities, and social structures. The timeline of human evolution includes several genera such as Ardipithecus, Australopithecus, Paranthropus, and Homo. Noteworthy species include Ardipithecus ramidus, Australopithecus afarensis 'Lucy,' Homo habilis, Homo erectus, Homo neanderthalensis (Neanderthals), and finally, Homo sapiens. The process of human evolution was influenced by factors such as migration, climate change, and genetic mutations, leading to the diverse populations and cultures that exist today."}</code> }
WebGPT	CoT	14K	-	-	{ <code>"instruction": "What causes that horrible screeching feedback sound when a microphone gets too close to a speaker?"</code> , <code>"input": "[TITLE] Why does my microphone make a loud screeching sound? (www.scienceabc.com)"</code> , <code>"output": "A typical audio system (like a Public Address system or the audio system used by bands) consists of three essential components: a microphone, a speaker and an amplifier. Wherever all three of these components are present, there is the potential for feedback. The reason is simple; feedback occurs when the microphone picks up the output sound from the speakers and then sends it back to the speakers to re-amplify it, kick-starting an endless loop unless interfered with externally."}</code> { <code>"instruction": "What causes that horrible screeching feedback sound when a microphone gets too close to a speaker?"</code> , <code>"input": "[TITLE] Why does my microphone make a loud screeching sound? (www.scienceabc.com)"</code> , <code>"output": "However, if the sound discharged from the speakers somehow reaches back to the mic (which ideally shouldn't happen), the process discussed above kick-starts again, i.e., the mic transmits sound to the amplifier, which then transmits to the speaker, and back to the mic... and then this goes on and on. The result is that you hear a high-pitched squeal, which gets louder and louder (due to the reinforced amplitude as a result of multiple rounds of amplification) until it is corrected."}</code> { <code>"instruction": "What Causes Microphone Feedback and How to Stop It - Virtuoso Central (virtuosocentral.com)"</code> , <code>"input": "[CONTEXT] Audio feedback happens when a sound coming out of a loudspeaker is picked up by the microphone reentering the sound system again and again in an always increasing loop. The result is a loud rumble or a high pitch ringing noise."}</code> , <code>"output": "Audio feedback occurs when the microphone picks up the output sound from the speakers and then sends it back to the speakers to re-amplify it, kick-starting an endless loop unless interfered with externally. [1] If the sound discharged from the speakers somehow reaches back to the mic, the process discussed above kick-starts again, i.e., the mic transmits sound to the amplifier, which then transmits to the speaker, and back to the mic... and then this goes on and on. The result is that you hear a high-pitched squeal, which gets louder and louder (due to the reinforced amplitude as a result of multiple rounds of amplification) until it is corrected. [2]"}</code> }

TABLE 8
Statistics of Datasets (Part 6).

Dataset	Task	Train	Val	Test	Example
Lima	CoT	1K	-	-	{ "instruction": "Can brain cells move? By movement I mean long distance migration (preferably within the brain only)."; "input": ""; "output": "The question is relatively broad and one should take into account that the brain not only consists of neurons, but also glial cells (supportive cells) and pre-mitotic neuronal stem cells. Furthermore, as critical fellow-scientists have indicated, developmental stage is very important, as the developing embryonic brain is very different from the adult brain.\nHowever, after sifting through various publications, the answer to the question is actually remarkably simple: Yes, brain cells migrate.\nIn the adult brain glial cells migrate in the brain (Kl\u00e4mbt, 2009). Glial cells are involved in a myriad of functions, but a notable example of migrating glial cells are the oligodendrocytes that migrate relative long distances to find their target axons onto which they wrap themselves to form the insulating myelin sheath (Tsai and Miller, 2002).\nNeuronal stem cells migrate over long distances in response to injury (Imitola et al., 2004) and they migrate from specific stem-cell locations (e.g., hippocampus and subventricular zone) to other regions (Clarke, 2003).\nPost-mitotic, but non-differentiated neurons have been shown to migrate in the adult brain in fish (Scott et al., 2012), and in mammals and non-human primates as well (Sawada et al., 2011).\nNot surprisingly, glial cells, stem cells and neurons also migrate during embryonic development. Most notably, post-mitotic neurons destined to fulfill peripheral functions have to migrate over relatively long distances from the neural crest to their target locations (Neuroscience, 2nd ed, Neuronal Migration)."} }
Code-Alpaca	Coding	20K	-	-	{ "instruction": "Create a Python program to accept a string from the user and print out the number of vowels in the string."; "input": "Hello World"; "output": "def countVowels(str):\n\tvowel = 0\n\tfor i in str: \n\t\tif i.lower() in ['a', 'e', 'i', 'o', 'u']: \n\t\t\tvowel += 1\n\treturn vowel \n\n# Driver code \nstr = \"Hello World\"\n\nprint(\"Number of vowels are:\", countVowels(str))"} }
Thought Source	CoT	343K	-	-	{ "instruction": "Two friends plan to walk along a 43-km trail, starting at opposite ends of the trail at the same time. If Friend P's rate is 15% faster than Friend Q's, how many kilometers will Friend P have walked when they pass each other?"; "input": "choices: 21,21.5,22,22.5,23"; "output": "If Q complete x kilometers, then P completes 1.15x kilometers.\nx + 1.15x = 43\n2.15x=43\nx = 43/2.15 = 20\nThen P will have have walked 1.15*20=23 km.\nThe answer is E.the answer is 23"} }
CAMEL-AI-Society	Society	107K	-	-	{ "instruction": "Create a function that can read in a PDF file."; "input": "File path to a PDF file."; "output": ""\nimport PyPDF2\n\ndef read_pdf(file_path):\n with open(file_path, 'rb') as pdf_file:\n pdf_reader = PyPDF2.PdfFileReader(pdf_file)\n text = ""\n for page in range(pdf_reader.getNumPages()):\n text += pdf_reader.getPage(page).extractText()\n return text\n\n\nThis function takes in a file path to a PDF file and returns the text content of the PDF file. It uses the PyPDF2 library to read in the PDF file and extract the text from each page. The extracted text is then concatenated and returned as a single string." }
CAMEL-Code	Coding	367K	0	0	{ "Instruction": "Implement a method to extract text from a PDF file using Apache PDFBox library."; "Input": "Path to the PDF file."; "output": "Solution: Here's a method that uses Apache PDFBox library to extract text from a PDF file:\n\nimport java.io.IOException;\nimport org.apache.pdfbox.pdmodel.PDDocument;\nimport org.apache.pdfbox.text.PDFTextStripper;\n\npublic String extractTextFromPDF(String filePath) throws IOException {\n PDDocument document = null;\n try {\n document = PDDocument.load(new File(filePath));\n PDFTextStripper stripper = new PDFTextStripper();\n return stripper.getText(document);\n } finally {\n if (document != null) {\n document.close();\n }\n }\n }\n\n\nThis method loads the PDF document from the specified file path, creates a PDFTextStripper object to extract the text, and returns the extracted text as a String. It also ensures that the document is properly closed after use. Next request." }
CAMEL-Math	Math	46K	0	0	{ "Instruction": "Solve for x: 5x + 3 = 28"; "Input": ""; "output": "To solve for x, we need to isolate x on one side of the equation. Step 1: Subtract 3 from both sides of the equation. 5x + 3 - 3 = 28 - 3 5x = 25 Step 2: Divide both sides of the equation by 5. 5x / 5 = 25 / 5 x = 5 So, x = 5." }

TABLE 8
Statistics of Datasets (Part 7).

Dataset	Task	Train	Val	Test	Example
CAMEL-Physics	Physics	20K	0	0	{ "Instruction": "What is the energy difference between the n=4 and n=2 energy levels of a hydrogen atom, and what is the frequency of the photon emitted when an electron transitions from the n=4 to n=2 energy level?"; "Input": ""; "output": "To find the energy difference between the n=4 and n=2 energy levels of a hydrogen atom, we can use the formula for the energy of an electron in a hydrogen atom: $E_n = -13.6 \text{ eV} / n^2$ where E_n is the energy of the electron in the nth energy level and n is the principal quantum number. First, let's find the energy of the electron in the n=4 energy level: $E_4 = -13.6 \text{ eV} / 4^2 = -13.6 \text{ eV} / 16 = -0.85 \text{ eV}$ Now, let's find the energy of the electron in the n=2 energy level: $E_2 = -13.6 \text{ eV} / 2^2 = -13.6 \text{ eV} / 4 = -3.4 \text{ eV}$ The energy difference between the n=4 and n=2 energy levels is: $\Delta E = E_4 - E_2 = -0.85 \text{ eV} - (-3.4 \text{ eV}) = 2.55 \text{ eV}$ Now, we need to find the frequency of the photon emitted when an electron transitions from the n=4 to n=2 energy level. First, we need to convert the energy difference from electron volts (eV) to joules (J): $1 \text{ eV} = 1.60218 \times 10^{-19} \text{ J}$ $\Delta E = 2.55 \text{ eV} \times 1.60218 \times 10^{-19} \text{ J/eV} = 4.08556 \times 10^{-19} \text{ J}$ Next, we can use the Planck's equation to find the frequency of the photon: $E = h \times f$ where E is the energy of the photon, h is the Planck's constant ($6.626 \times 10^{-34} \text{ Js}$), and f is the frequency of the photon. Rearranging the equation to solve for the frequency: $f = E / h = (4.08556 \times 10^{-19} \text{ J}) / (6.626 \times 10^{-34} \text{ Js}) = 6.165 \times 10^{14} \text{ Hz}$ So, the frequency of the photon emitted when an electron transitions from the n=4 to n=2 energy level is approximately $6.165 \times 10^{14} \text{ Hz}$." }
CAMEL-Chemistry	Chemistry	20K	0	0	{ "Instruction": "What is the IUPAC name for the organic compound with the molecular formula C6H12O2?"; "Input": ""; "output": "There can be several isomers with the molecular formula C6H12O2, so it is not possible to provide a specific IUPAC name without more information about the structure of the compound. If you can provide the structure or any additional details, I would be happy to help you determine the IUPAC name." }
CAMEL-Biology	Biology	20K	0	0	{ "Instruction": "What are the common techniques used in identifying a new species, and how can scientists accurately categorize it within the existing taxonomy system?"; "Input": ""; "output": "Identifying a new species and categorizing it within the existing taxonomy system involves several common techniques. These techniques can be broadly classified into morphological, molecular, and ecological approaches. Here's an overview of these techniques: 1. Morphological analysis: This is the traditional method of identifying a new species based on its physical characteristics. Scientists examine the external and internal features of an organism, such as its size, shape, color, and structure. They also study the anatomy and physiology of the organism, including its skeletal, muscular, and reproductive systems. By comparing these features with those of known species, scientists can determine if the organism represents a new species. 2. Molecular analysis: With advances in molecular biology, scientists can now use genetic information to identify and classify new species. This involves analyzing the DNA or RNA sequences of the organism and comparing them with the sequences of known species. Techniques such as DNA barcoding, which compares a short, standardized region of the genome, can help determine if the organism is a new species. Additionally, phylogenetic analysis can be used to understand the evolutionary relationships between the new species and other known species, helping to place it within the existing taxonomy system. 3. Ecological analysis: Studying the ecological niche of an organism can also provide valuable information for species identification and classification. This involves examining the organism's habitat, its interactions with other species, and its role in the ecosystem. By understanding the ecological context of the new species, scientists can better determine its taxonomic position and how it relates to other known species. 4. Behavioral analysis: Observing the behavior of an organism can also help in identifying a new species. This includes studying its feeding habits, mating rituals, and social interactions. Behavioral differences between closely related species can sometimes be more apparent than morphological or molecular differences. 5. Biogeography: The geographical distribution of an organism can provide clues about its evolutionary history and help in its classification. Studying the biogeography of a new species can reveal patterns of speciation and help determine its taxonomic position. Once a new species has been identified using these techniques, scientists can accurately categorize it within the existing taxonomy system by following the principles of biological classification. This involves placing the new species within a hierarchical structure of taxonomic ranks, such as kingdom, phylum, class, order, family, genus, and species. The new species is then given a scientific name, usually consisting of a genus name and a species epithet, following the rules of binomial nomenclature. In conclusion, identifying a new species and categorizing it within the existing taxonomy system involves a combination of morphological, molecular, ecological, behavioral, and biogeographical analyses. By using these techniques, scientists can accurately classify the new species and better understand its evolutionary relationships with other organisms." }

TABLE 9
Evaluation results of all LLaMA2 models in the LoRA bank.

Model	ARC-c	ARC-e	GSM8K	MBPP	BoolQ	PiQA	Average
Base	33.90%	49.91%	16.68%	18.20%	47.86%	53.05%	29.67%
ARC-c	44.07%	59.44%	15.54%	23.80%	43.33%	56.42%	35.71%
ARC-e	47.12%	62.61%	16.98%	24.60%	48.13%	58.11%	37.83%
WinoGrande	26.61%	53.26%	16.98%	23.60%	62.14%	56.09%	30.11%
GSM8K	20.81%	14.58%	22.88%	21.20%	18.53%	52.61%	19.87%
PiQA	37.97%	53.26%	17.51%	22.40%	42.51%	56.58%	32.79%
CommonSenseQA	37.29%	49.38%	16.38%	23.20%	46.18%	51.80%	31.56%
RACE	49.49%	69.31%	17.29%	21.40%	65.81%	55.55%	39.37%
MBPP	31.19%	46.56%	16.22%	22.40%	43.18%	52.77%	29.09%
MathQA	34.92%	49.03%	15.09%	21.80%	58.07%	53.65%	30.21%
Esnli	20.34%	27.34%	13.57%	21.40%	36.88%	44.45%	20.66%
ECQA	13.22%	13.58%	15.16%	21.80%	0.64%	35.15%	15.94%
CREAK	30.17%	34.22%	15.54%	21.20%	22.35%	56.53%	25.28%
GPT4Tools	25.76%	37.04%	17.29%	20.80%	31.87%	46.84%	25.22%
AQuA	39.32%	53.79%	15.31%	21.20%	64.77%	56.91%	32.41%
QASC	35.25%	42.33%	15.47%	21.60%	27.28%	55.66%	28.66%
QED	10.51%	14.99%	14.56%	21.60%	5.20%	35.91%	15.42%
StrategyQA	35.25%	45.50%	15.24%	20.40%	43.70%	56.37%	29.10%
SensemakingQA	19.66%	20.46%	15.16%	20.00%	34.95%	48.31%	18.82%
Toolformer	32.54%	36.86%	18.35%	19.00%	35.66%	51.80%	26.69%
HellaSwag	35.59%	50.79%	18.50%	23.20%	59.76%	45.27%	32.02%
SiQA	36.95%	49.74%	13.72%	18.20%	59.42%	56.53%	29.65%
BoolQ	36.61%	54.32%	9.48%	24.20%	63.39%	45.43%	31.15%
Dolly	31.19%	40.21%	17.21%	22.40%	15.84%	53.97%	27.75%
WizardLM	38.98%	49.38%	16.38%	16.00%	21.77%	50.98%	30.19%
ShareGPT	41.36%	55.38%	15.62%	18.20%	34.59%	53.97%	32.64%
GPT-Teacher-Code	34.58%	46.56%	18.50%	21.40%	46.88%	54.73%	30.26%
GPT-Teacher-Roleplay	35.25%	46.91%	17.51%	23.80%	40.64%	53.32%	30.87%
GPT-Teacher-Instruct	35.43%	48.93%	17.01%	21.20%	42.02%	55.28%	30.64%
WebGPT	32.88%	44.09%	14.40%	19.80%	30.89%	49.46%	27.79%
Lima	30.52%	39.51%	16.00%	21.20%	15.78%	50.65%	26.81%
Code-Alpaca	33.56%	44.80%	16.07%	21.80%	33.03%	51.69%	29.06%
ThoughtSource	35.59%	51.32%	20.85%	21.20%	54.98%	61.53%	32.24%
CAMEL-AI-Society	31.86%	41.09%	16.53%	19.40%	25.99%	43.04%	27.22%
CAMEL-Code	26.10%	23.99%	1.67%	1.00%	29.42%	40.86%	13.19%
CAMEL-Math	33.90%	48.32%	17.44%	22.80%	45.29%	50.00%	30.62%
CAMEL-Physics	26.78%	39.33%	15.24%	24.40%	32.08%	49.73%	26.44%
CAMEL-Chemistry	34.58%	40.74%	17.66%	24.20%	26.73%	48.37%	29.30%
CAMEL-Biology	31.53%	41.62%	17.59%	22.60%	31.93%	50.44%	28.34%

TABLE 10
Evaluation results of all Mistral models in the LoRA bank.

Model	ARC-c	ARC-e	GSM8K	MBPP	BoolQ	PiQA	Average
Base	60.68%	73.54%	45.56%	36.00%	55.96%	57.67%	54.90%
ARC-c	77.97%	88.36%	47.23%	40.20%	67.55%	64.85%	64.36%
ARC-e	80.00%	90.30%	51.55%	40.60%	59.39%	60.34%	63.70%
WinoGrande	61.69%	78.84%	47.54%	39.80%	69.30%	54.79%	58.66%
GSM8K	49.83%	63.84%	49.73%	36.80%	11.19%	58.27%	44.94%
PiQA	76.27%	87.83%	47.99%	40.60%	78.78%	68.12%	66.60%
CommonSenseQA	75.25%	81.31%	49.20%	40.40%	61.68%	65.02%	62.14%
RACE	74.92%	86.42%	48.67%	39.00%	74.53%	71.76%	65.88%
MBPP	65.08%	60.34%	44.88%	37.60%	48.56%	57.02%	52.25%
MathQA	73.90%	83.42%	43.52%	35.40%	76.79%	63.60%	62.77%
Esnli	43.05%	55.37%	31.92%	34.60%	0.49%	49.56%	35.83%
ECQA	60.00%	65.26%	36.92%	36.00%	5.78%	58.71%	43.78%
CREAK	68.81%	71.43%	42.99%	38.20%	6.06%	66.97%	49.08%
GPT4Tools	69.15%	75.13%	46.70%	38.00%	60.49%	58.49%	57.99%
AQuA	68.74%	77.78%	41.32%	38.00%	45.93%	64.15%	55.99%
QASC	72.20%	78.66%	39.65%	35.80%	16.33%	68.66%	51.88%
QED	71.86%	66.78%	39.27%	37.20%	50.55%	66.76%	55.40%
StrategyQA	72.88%	80.78%	43.06%	38.40%	64.56%	65.56%	60.87%
SensemakingQA	38.31%	46.91%	38.82%	35.20%	1.83%	56.42%	36.25%
Toolformer	69.49%	76.01%	45.64%	38.00%	54.07%	59.58%	57.13%
HellaSwag	77.63%	88.01%	47.23%	40.20%	67.37%	67.79%	64.71%
SiQA	74.24%	81.83%	47.99%	38.20%	54.01%	65.56%	60.31%
BoolQ	73.22%	87.13%	46.78%	39.20%	80.12%	61.04%	64.58%
Dolly	73.56%	83.07%	46.47%	38.80%	48.99%	66.38%	59.55%
WizardLM	73.90%	79.37%	46.63%	36.60%	70.67%	63.60%	61.80%
ShareGPT	69.83%	78.66%	45.64%	37.00%	68.50%	68.61%	61.37%
GPT-Teacher-Code	66.78%	76.37%	47.01%	40.20%	57.22%	59.25%	57.81%
GPT-Teacher-Roleplay	66.78%	74.07%	49.43%	37.60%	67.06%	63.22%	59.69%
GPT-Teacher-Instruct	72.54%	79.72%	47.16%	37.60%	78.20%	64.74%	63.33%
WebGPT	63.39%	76.37%	43.21%	36.40%	52.91%	59.09%	55.23%
Lima	69.83%	77.43%	45.34%	37.80%	30.52%	56.64%	52.93%
Code-Alpaca	71.53%	79.89%	45.72%	40.00%	44.56%	62.40%	57.35%
ThoughtSource	77.97%	83.77%	45.49%	37.00%	78.38%	70.95%	65.59%
CAMEL-AI-Society	68.81%	77.07%	44.66%	38.00%	57.58%	63.49%	58.27%
CAMEL-Code	75.59%	79.54%	45.94%	37.80%	46.67%	65.23%	58.46%
CAMEL-Math	77.97%	84.30%	46.02%	38.80%	58.65%	60.01%	60.96%
CAMEL-Physics	71.86%	79.01%	46.78%	38.20%	51.01%	58.60%	57.58%
CAMEL-Chemistry	70.51%	80.42%	46.70%	38.40%	54.89%	60.72%	58.61%
CAMEL-Biology	63.73%	73.90%	47.16%	37.00%	52.02%	56.86%	55.11%

TABLE 11
List of symbols.

Symbol	Description
x	an input sequence (i.e., instruction) consisting of multiple tokens $x_{(i)}, i = 1, 2, \dots, x $
y	an output sequence (i.e., response) consisting of multiple tokens $y_{(i)}, i = 1, 2, \dots, y $
$x_{(i)}$	the i -th token of x
$y_{(i)}$	the i -th token of y
$y_{(<i)}$	the sequence of $y_{(j)}, j < i$, i.e., $[y_{(1)}, y_{(2)}, \dots, y_{(i-1)}]$
m	a LLM model from the LoRA bank
θ_m	the parameters of m
$P(y_{(i)} x, y_{(<i)}; \theta_m)$	the model m 's probability of the output token $y_{(i)}$ given the input x and the preceding output tokens $y_{(<i)}$
\hat{y}	the expanded output of y with CoT rationales
$\mathcal{L}(x, y, \theta_{\text{MoE}})$	the cross-entropy language modeling loss of the MoE system on y given x
$\text{PPL}(x, y, \theta_m)$	the perplexity of the model m parameterized by θ_m on the sequences y given x
$\Phi(\cdot, \cdot)$	the CoT expansion process implemented with prompts
K	the number of human-annotated instructions from tasks of interest
D_K	K -shot data from the task of interest: $\{(x_1, y_1), (x_2, y_2), \dots, (x_K, y_K)\}$
$\text{PPL}(x, \hat{y}, \theta_m)$	the reasoning perplexity of the model m parameterized by θ_m on the CoT-formatted \hat{y} given x
PPL_R	the total reasoning perplexity of the model m on D_K
$f(\cdot)$	the post-processing function for standardization of model responses
$\text{Acc}(m, D_K, f)$	the performance of the model m on D_K in exact match accuracy with a post-processing function $f(\cdot)$
\tilde{y}	the auto-regressively generated sequence given x
\tilde{y}'	the post-processed response of \tilde{y}
$\mathbb{1}(\cdot)$	the indicator function
B	the model bank consists of multiple models $\{m_1, m_2, \dots, m_{ B }\}$
M	the number of candidate models
B_M	a set of candidate models $B_M \subset B$
$\mathbf{E}(m_i)$	the flattened matrices of all layers of m_i
N	the number of experts
B_N	a set of chosen experts $B_N \subset B_M$
Ω_{B_N}	the intra-group diversity of B_N
$\text{rank}(\cdot)$	the ranking of models by certain indices
$R_L(m)$	the rank of the model m by $\mathcal{L}(m, D_K)$ from smallest to largest
$R_P(m)$	the rank of the model m by $\text{Acc}(m, D_K, f)$ from largest to smallest
$R_D(B_N)$	the rank of the N -tuple B_N by intra-group diversity Ω_{B_N} from the largest to the smallest
B_E	the chosen experts for initialization of a MoE system
w_i	the weight of the i -th LoRA module for linear composition of model merging
\mathbf{W}	the original parameter of a pre-trained model
$\Delta \mathbf{W}_i$	the i -th LoRA variant with $\sum_{i=1}^N w_i = 1$
$g^l(x)$	the output of a N -expert MoE system at the l -th layer given input x
$G^l(x)$	the gating vector at the l -th layer with $G^l(x) \in \mathbb{R}^N$ given x
$G_i^l(x)$	the i -th element of the gating vector $G^l(x)$
$g_i^l(x)$	the output from the i -th expert at the l -th layer
W_g^l	the matrix of a single fully-connected layer for the gating network
k	the number of the selected experts in a MoE system
$\text{top-}k(\cdot)$	the operation that returns the largest k elements unchanged and the other elements as $-\infty$
D_S	a set of S open-source samples: $\{(x_1, y_1), (x_2, y_2), \dots, (x_S, y_S)\}$
h	a pre-trained encoding model
θ_h	the parameters of the pre-trained model h
u_i	the embedding of both input and output $[x_i, y_i]$
U_K	the embeddings of samples in D_K
U_S	the embeddings of samples in D_S
D_C	the candidate open-source instruction set $D_C \subset D_S$
C	the budget for the candidate dataset D_C
$d(\cdot, \cdot)$	the distance function
$\text{sim}(\cdot, \cdot)$	the similarity metric
A_{ij}	the entry of the cross-dataset similarity matrix between each pair of $u_i \in U_K$ and $u_j \in U_S, A \in \mathbb{R}^{K \times S}$
I_{ij}	the entry of the intra-dataset similarity matrix between $u_i \in U_C$ and $u_j \in U_C, U_C = \{u_i (x_i, y_i) \in D_C\}$
τ	the threshold for semantic deduplication
D_A	the chosen open-source dataset for data augmentation
D_T	the official training set from the downstream task of interest (only involved in ablation studies)
U_K^C	the convex hull of the embeddings U_K from the K -shot data D_K
λ_i	the coefficients that determine the convex combination of samples in U_K
$\text{Ker}(\cdot)$	the kernel function for distance measurement
γ	the bandwidth controlling the smoothness of the density function
$p(u)$	the estimated density probability of a sample u in the embedding space

TABLE 12
List of hyper-parameters for training settings.

Settings	LoRA Models (Single)	MoE System
Optimizer	AdamW	
Optimizer momentum	0.9	
Optimizer weight decay	1×10^{-4}	
Batch size	2	
Gradient accumulation steps	16	
Training scheduler	Cosine decay with linear warm-up	
Learning rate	5e-5	
Transformers Version	4.36.1	
Location of PEFT	q_proj, v_proj	
Cutoff length	1024	
Deepspeed	Stage 3	
Training epochs in total	3	5